The TPenA Binding Site in TREK-1 Channels

Dissertation
zur Erlangung des akademischen Grades
doctor medicinae (Dr. med.)

vorgelegt dem Rat der Medizinischen Fakultät der Friedrich-Schiller-Universität Jena

von Paula Louise Piechotta

geboren am 19.09.1986 in Gera

Gutachter

1. Prof. Dr. Thomas Zimmer, Institut für Physiologie II, FSU Jena
2. Prof. Dr. Thomas Baukrowitz, Institut für Physiologie,
3. Prof. Dr. Ralf Mrowka, Klinik für Innere Medizin III, Universitätsklinikum Jena

Tag der öffentlichen Verteidigung: 05.05.2015

Table of Contents

Abbreviations

aka	also known as
4-AP	4-aminopyridine
ATP	adenosine triphosphate
BC	(helix) bundle crossing
BK	big potassium channels
CNG	cyclic nucleotide-gated channels
cRNA	ribonucleic acid derived from complementary deoxyribonucleic acid
Cs^+	Caesium
DAG	diacylglycerol
D_{2D}	planar conformation of a TnA molecule
dl	deciliter
EC_{50}	half maximal effective concentration
EGTA	ethylene glycol tetraacetic acid
fig.	figure
fMRI	functional magnetic resonance imaging
GFG	glycine-phenylalanine-glycine
GYG	glycine-tyrosine-glycine
$\Delta\Delta G_{INT}$	interaction free energy
Gq	heterotrimeric G-protein subunit activating phospholipase C
HDAC5	gene encoding histone deacetylase
HEPES	4-(2-hydroxyethyl)-1-piperazineethanesulfonic acid
hERG	voltage-gated potassium channel subfamily H member 2, also: ether-a-go-go-related gene potassium channel 1
$5\text{-}HT_{1B}$	5-hydroxytryptamine receptor 1B
IC_{50}	half maximal inhibitory concentration
I_{max}	maximum current
IP_3	inositol-3-phosphate
K	Kelvin
K^+	Potassium
kHz	kilohertz
LPC	lysophosphatidylcholine

KcsA	*Streptomyces lividans* K^+ channel
KCNK2	gene encoding TREK-1
KCNKØ	gene encoding a K2P channel in *Drosophila melanogaster*, also: ORK1
K_{ir}	inward rectifying Potassium channels
K2P	two-pore domain potassium channels
KvAP	voltage-gated potassium channel from *Aeropyrum pernix*
Kv1.2	voltage-gated potassium channel subfamily A member 2
k_{on}	on-rate of blocker binding
K_v	voltage-gated potassium channels
MD	molecular dynamics
mg	milligram
MlotiK	bacterial cyclic nucleotide-regulated channel
mM	millimolar
µM	micromolar
MΩ	megaohm
ms	millisecond
MthK	Calcium-gated potassium channel in *Methanothermobacter thermautotrophicus*
mRNA	messenger ribonucleic acid
mV	millivolt
nA	nanoampere
Na^+	Sodium
NaK	nonselective cation channel from *Bacillus cereus*
$NaPP_i$	sodium pyrophosphate
ORK1	K2P channel in *Drosophila melanogaster,* also: KCNKØ
P1	first pore loop
P2	second pore loop
pH	decimal logarithm of the reciprocal of the hydrogen ion activity
pH_{ic}	intracellular pH
PIP_2	phosphatidylinositol 4,5-bisphosphate
PI_4P	phosphatidyl-4-phosphate
pK_A	acid dissociation rate
PKA	protein kinase A
PKC	protein kinase C

PKG	protein kinase G
P_o	open probability
pS	picosiemens
PUFA	polyunsaturated fatty acids
PVP	proline-valine-proline
PXP	proline-X-proline
QA	quaternary ammonium compounds
R	gas constant
Rb^+	Rubidium
RNA	ribonucleic acid
rTREK-1	rat homolog of TREK-1
S6	sixth transmembrane helix in subunits of voltage-gated potassium channels
S100A10	gene encoding the protein p11
SD	standard deviation
SEM	standard error of the mean
SLC18A2	gene encoding vesicular monoamine transporter 2
SNP	single-nucleotide polymorphism
STAR*D	„Sequenced Treatment Alternatives to Relieve Depression" clinical study
T	temperature
TALK	TWIK-related alkaline pH-activated K^+ channel
TBA	tetrabutylammonium bromide
TEA	tetraethylammonium
TEA-C9	nonyltriethylammonium
THepA	tetraheptylammonium bromide
THexA	tetrahexylammonium chloride
THIK	Halothane-Inhibited K^+ Channel
Tl^+	Thallium
TM	transmembrane helix
2TM-1P	potassium channels in which each subunit contains two transmembrane helices (2TM) and one pore loop (1P)
TnA	derivatives of tetraethyl ammonium with n-alkylic side chains
TOA	tetraoctylammonium chloride

τ_{on}	open time constant of blocker binding
TPenA	tetrapentylammonium chloride
TREK	TWIK-related K^+ Channel
TRESK	TWIK-related spinal cord K^+ channel
TASK	TWIK-related acid sensing K^+ channel
TRAAK	TWIK-related arachidonic acid-stimulated K^+ channel
TRPV1	transient receptor potential cation channel subfamily V member 1
TWIK	weak inward rectifying K^+ channel
VMD	Visual molecular dynamics, molecular graphics software
WT	wild-type

1 Summary

Two-pore domain potassium channels (K2P) represent an ion channel family of vital importance to cell excitability, maintaining background potassium currents beyond the K^+ conductance provided by inward rectifying potassium channels (K_{ir}). TREK-1 as the most intensively studied member is tightly regulated by an abundance of stimuli, including pH, lipids, pressure, temperature and voltage. Moreover, it has been linked to the pathophysiology of depression and epilepsy as well as to the onset of anesthesia. Being discovered recently, its architecture and structure-function relationships are only vaguely understood despite its remarkable physiological relevance.

In this study, a new class of K2P blockers, derivatives of tetraethyl ammonium (TEA) with longer alkylic side chains (TnA) is described. Their binding site is determined by site-directed mutagenesis and inside-out giant patch recordings. Experiments on the inhibitory mechanism of TEA derivatives in TREK-1 channels are shown, which reveal that these molecules act as open channel blockers, similar to their mode of action in other channel families like voltage-gated potassium channels.

Furthermore, it is demonstrated that unlike the majority of K^+ channels, TREK-1 does not possess an intracellular gate controlling the intracellular entrance into the channel cavity, but is rather characterized by being constitutively open on its cytosolic side.

This missing lower gate implies the necessity of an alternative gating mechanism located in a different region of the protein, very close to or within the selectivity filter region. Such a gate is supported by two lines of evidence in this study: First, mutated residues very close to the selectivity filter region dramatically affect pH gating, either in- or decreasing pH sensitivity. Second, exchanging the permeant ion influences pH sensitivity as well, with rubidium ions shifting pH activation to less acidic pH and Thallium ions shifting it to higher pH values.

A similar gating concept has already been proposed to be the primary gating mode in CNG channels (Contreras und Holmgren 2006, Contreras et al. 2008) and given the

recent literature on BK channels it might not be unprecedented in the class of potassium channels either (Chen und Aldrich 2011).

The results of this study have been published in:

*Piechotta PL, Rapedius M, Stansfeld PJ, Bollepalli MK, Ehrlich G, Andres-Enguix I, Fritzenschaft H, Decher N, Sansom MS, Tucker SJ, Baukrowitz T. 2011. **The pore structure and gating mechanism of K2P channels.** EMBO J, 30 (17):3607-3619.*

Zusammenfassung

Kalium-Zwei-Poren-Kanäle (K2P) stellen eine Ionenkanal-Familie mit großer Bedeutung für das zelluläre Ruhemembranpotential dar, da sie gemeinsam mit der Kanalfamilie der Kalium-Einwärtsgleichrichter (K_{ir}) die Ruheleitfähigkeit für Kaliumionen gewährleisten. TREK-1 ist der am intensivsten untersuchte Vertreter der K2P-Kanäle und wird stark reguliert durch eine Vielzahl physiologischer Stimuli, die pH, Lipide, mechanischen Druck, Temperatur und elektrische Spannung umfassen. Darüber hinaus ist er in die Pathophysiologie von depressiven Erkrankungen und Epilepsie sowie das Ansprechen auf Anästhetika eingebunden. Trotz dieser potentiell enormen physiologischen und pathophysiologischen Relevanz dieses Kanalproteins sind sein Aufbau und das Zusammenspiel von Struktur und Funktion nur schemenhaft verstanden.

In der vorliegenden Arbeit wird eine neue Klasse von porenblockierenden Molekülen an K2P-Kanälen beschrieben, die TEA-Derivate mit verlängerten Alkyl-Seitenketten darstellen (TnA). Mithilfe von Mutagenese und sogenannten „inside-out giant patches" konnte außerdem die Bindungsstelle dieser Moleküle in der Pore des TREK-1-Kanals identifiziert werden. Weitere Experimente zum Inhibitionsmechanismus zeigen anschließend, dass TnA-Moleküle in K2P-Kanälen als Blocker der offenen Kanalpore fungieren und dieser Inhibitionsmechanismus jenem von TEA in anderen Kaliumkanalfamilien wie spannungsgesteuerten Kaliumkanälen vergleichbar ist. Des Weiteren wird gezeigt, dass im Gegensatz zu anderen Kaliumkanalfamilien im TREK-1-Kanal kein zytosolischer Schließmechanismus (gate) das Öffnen

und Schließen des Kanalproteins reguliert. Vielmehr ist das zytosolische gate des Kanals immer geöffnet.

Das Fehlen des zytosolischen Schließmechanismus impliziert, dass Öffnen und Schließen des Kanals von einem anderen Mechanismus gewährleistet werden. Dafür wird in dieser Arbeit ein „Selektivitätsfilter-Gate" hypothetisiert, in dem das Schließen des Kanals durch ein temporäres Kollabieren des Selektivitätsfilters erklärt wird. Diese Hypothese wird gestützt durch zwei experimentelle Ergebnisse: Erstens führen Mutationen in direkter Nähe zum Selektivitätsfilter zu deutlichen Veränderungen in der Aktivierbarkeit des TREK-1-Kanals. Zweitens können ebenfalls deutliche Änderungen dieser Aktivierbarkeit erzeugt werden durch ein Ersetzen des permeierenden Kalium-Ions durch Thallium- oder Rubidium-Ionen. Dabei führt Rubidium zu einem Absinken des halbmaximalen pH-Wertes für eine pH-Aktivierung, während Thallium-Ionen diesen erhöhen. Ein ähnliches Konzept des sogenannten „gatings", also des Öffnens und Schließens eines Kanals, das nur auf Mechanismen im Selektivitätsfilter beruht, wurde bereits für CNG-Kanäle postuliert (Contreras und Homgren 2010, Contreras et al. 2008). Vor dem Hintergrund neuerer Literatur zur BK-Kaliumkanälen könnte es darüber hinaus auch in anderen Kaliumkanälen von Bedeutung sein (Chen und Aldrich 2011).

Die Ergebnisse der vorliegenden Arbeit wurden publiziert in:

Piechotta PL, Rapedius M, Stansfeld PJ, Bollepalli MK, Ehrlich G, Andres-Enguix I, Fritzenschaft H, Decher N, Sansom MS, Tucker SJ, Baukrowitz T. 2011. **The pore structure and gating mechanism of K2P channels.** *EMBO J, 30 (17):3607-3619.*

2 Introduction

2.1 The K2P family

After it had been hypothesized in the 1940s, that mechanisms allowing potassium ions to leak out of the cell must exist (Goldman 1943, Hodgkin und Huxley 1947), until 1996 the molecular counterpart maintaining that process was believed to be solely resembled by inward rectifying K^+ channels. In that year, the first protein of the K2P family was discovered (Lesage et al. 1996), which was followed by 14 other members in six subfamilies (table 1).

The then discovered K2P channels are dimers, with each subunit consisting of four transmembrane helices (TM1 - 4) and two pore loop forming segments (P1 and P2). The latter contain the crucial feature for potassium selectivity, the G(Y/F/L)G motif of the filter. Whereas this filter is highly conserved in classical potassium channels as T-

Table 1. The subfamilies and 14 members of the K2P channel family along with their first mention in the scientific literature.

TWIK (weak inward rectifying K^+ channel)	TWIK1	(Lesage et al. 1996)
	TWIK2	(Chavez et al. 1999)
TREK (TWIK-related K^+ channel)	TREK1	(Fink et al. 1996)
	TREK2	(Bang et al. 2000)
		(Lesage et al. 2000)
	TRAAK	(Fink et al. 1998)
TASK (TWIK-related acid sensing K^+ channel)	TASK1	(Duprat et al. 1997)
	TASK3	(Rajan et al. 2000, Kim et al. 2000)
	TASK5	(Kim und Gnatenco 2001, Ashmole et al. 2001)
TALK (TWIK-related alkaline pH-activated K^+ channel)	TALK1	(Girard et al. 2001)
	TALK2	(Girard et al. 2001)
	TASK2	(Reyes et al. 1998)
THIK (Halothane-inhibited K^+ channel)	THIK1	(Rajan et al. 2001)
	THIK2	(Rajan et al. 2001, Girard et al. 2001)
TRESK (TWIK-related spinal cord K^+ channel)	TRESK	(Sano et al. 2003)

X-G-Y-G-D, in K2P channels this motif shows greater variation and only two con–served residues: T-X-G-X-X. With two different pore loop forming segments in each subunit, K2P channels feature asymmetrical pores, while classic potassium channels are known to show fourfold symmetry. This implies that in any standard site-directed mutagenesis scan done on K2P channels, only two altered residues will be intro–duced into the channel. This is contrary to site directed mutagenesis in tetrameric K_{ir} and K_v channels - in these, mutagenesis results in four effectively mutated residues per channel. The unusual length of the first pore loop P1 in K2P channels, but not the second pore loop, represents one more distinction between them and classical potassium channels with their shorter and fourfold symmetrical extracellular pore loops.
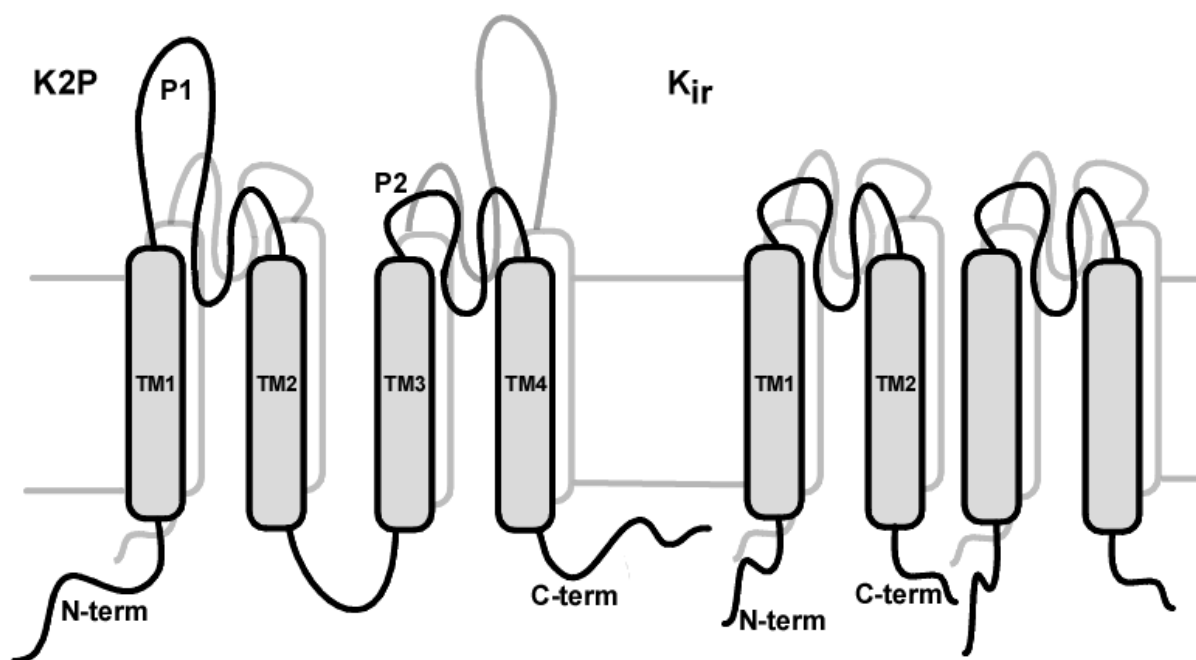

Figure 1. *Structural differences between K2P and K_{ir} channels.* In K2P channels, each subunit consists of four transmembrane helices (TM1 – 4) and two different pore forming loops (P1 and P2). Combining two subunits results in the two-fold symmetry of the assembled protein. In tetrameric K_{ir} channels, each channel includes four subunits. Therefore, subunits only contain one pore loop region, and the channel protein displays fourfold symmetry.

Common features in the K2P family include the ability to conduct background currents (Enyedi und Czirjak 2010) and multiple channel regulation pathways besides voltage dependence. Due to their properties, K2P channels are of vital importance to the cell's resting potential and its control of potassium homeostasis. Correspondingly, they are expressed ubiquitously in the human body.

2.2 Molecular and biophysical properties of TREK-1

The gene KCNK2 encodes a TREK-1 channel subunit of 426 residues. Two different splice variants have been reported (Xian Tao et al. 2006) as well as two different protein isoforms caused by alternative translation initiation (Thomas et al. 2008).

Previously, the TREK-1 channel was reported to show a single channel conductance of 101 ± 3 pS under symmetrical K^+ conditions, given a membrane potential of 50 mV (Patel et al. 1998b). Furthermore, Bockenhauer et. al. demonstrated that TREK-1 displays one open state and two distinct closed states at − 60 mV. Phosphorylation affects one of two closed states: Its dwell time of 6.1 ± 1.0 ms in the dephosphorylated state switches to a dwell time of 1700 ± 2000 ms upon the treatment with protein kinase A and ATP (Bockenhauer et al. 2001).
Additionally, later investigations described two different conductance modes (Xian Tao et al. 2006), that are unaffected by different splicing variants.

2.3 Regulation of TREK-1

Prior to the discovery of the K2P channel family, the simplest model of „potassium leak channels" resembled constitutively open, unregulated pores. However, soon after the characterisation of K2P channels it became obvious that, in agreement with their considerable effect on the resting potential of every cell, they are in fact tightly regulated.

With multiple regulation pathways being described for two-pore domain channels, the plethora of currently known mechanisms affecting the activity of TREK-1 is un–equalled even in this protein family. Voltage, pH, lipids, temperature, mechanical

stress and phosphorylation have been reported to influence channel gating. How-ever, compared to the rest of the family, this multitude of gating factors might be partly explicable in terms of TREK-1 being the most intensively studied K2P member thus far.

Voltage dependency. Given symmetrical potassium concentrations, TREK-1 shows pronounced outward rectification and is usually considered to classify as an outward rectifier. However, this voltage dependency in TREK-1 can be overruled via protein dephosphorylation of a serine at position S333 or treatment with phosphatidylinositol-4,5-bisphosphate (PIP_2). Both convert TREK-1 into an open leak channel (Bockenhauer et al. 2001, Chemin et al. 2005b). Inversely, phosphorylation of S333 by protein kinase A (PKA) is necessary for outward rectification. This regulation requires the TREK-1 „proton sensor" glutamic acid E321 to be intact (Honore et al. 2002a).

Intracellular pH-sensitivity. TREK-1 channels are regulated by protons from the intra-cellular side of the membrane in a reversible and dose-dependent manner (Honore et al. 2002a). Cytosolic acidification stabilizes the open state of the channel. In the first paper describing TREK-1 pH sensitivity, one single residue, the above-mentioned proton sensor E321, was shown to be essential for intracellular pH activation. Introducing hydrophobic or positively charged mutants at this position like E306A increases the open probability (P_o) of the channel remarkably as it mimicks a proton-ated glutamine acid. At the same time, these mutations render the channel immune to further mechanical or lipid activation. Interestingly, protonating the native glutamate resulted in higher pressure sensitivity, shifting the half maximum activation pressure to less negative values. No effect was detected upon introducing the con-servative mutation E321D. Furthermore, Chemin et al. described a „locked open state" of the channel: When they added phospholipids and decreased the intra-cellular pH (pH_{ic}), TREK-1 channels were irreversibly transformed into open leak channels, which were no longer sensitive to many usual regulatory stimuli including pH_{ic} whereas pressure regulation was preserved (Chemin et al. 2005b). Therefore, Honoré et al. proposed a functional model that focuses on the interaction between the proximal C-terminus including E321 and the negatively charged phospholipids like PIP_2 within the inner bilayer (Fig. 2). Glutamate E321 as a negatively charged

amino acid is embedded in a cluster of five positively charged residues, namely R312, K316, K317, K319 and R326. The authors hypothesized, that the interaction between this „positive stretch" and the inner membrane leaflet can be prevented in the presence of glutamate E321.
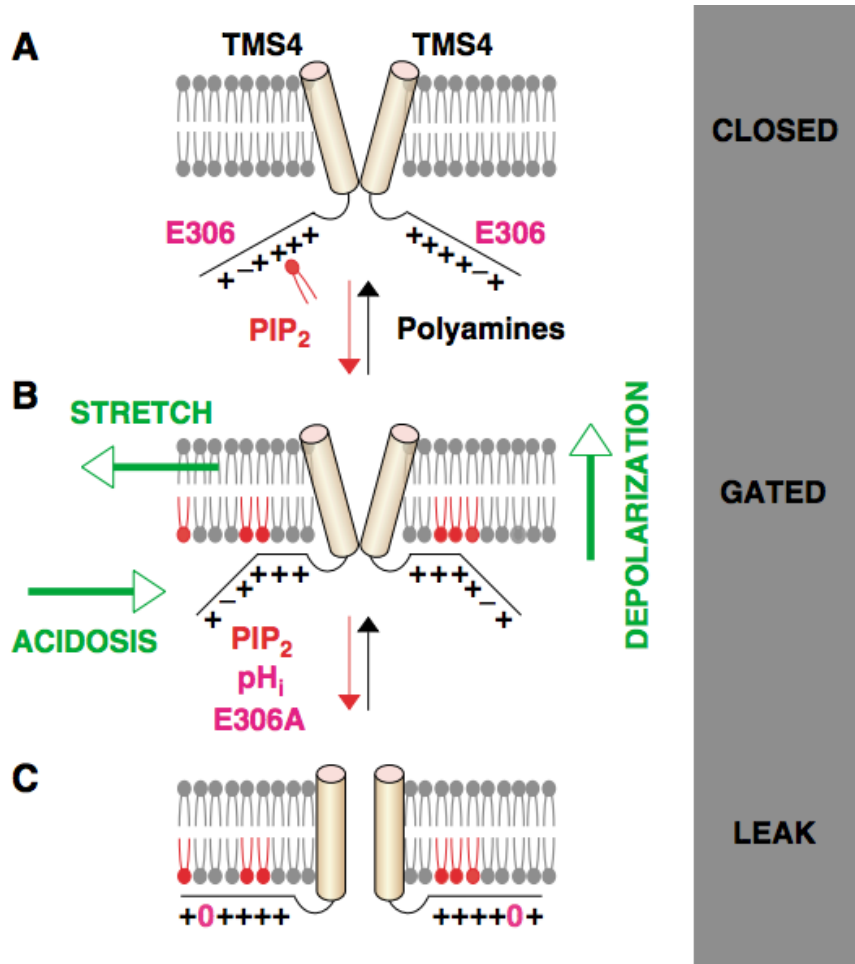

Figure 2. *The proton sensor E321 (E306) controls gating in TREK-1 channels (Chemin et al. 2005b).* Please note, that due to different counting in the original paper, E321 is named E306 in this figure. (A) When positively charged polyamines like spermine or polylysine are applied, negatively charged phospholipids like PIP_2 are cleaved and cannot interact with the cytosolic domain of TREK-1. (B) In the presence of PIP_2 in the inner membrane leaflet, the cytosolic C-terminus can interact with the membrane and hence force conformational changes upon the channel protein. In this state, TREK-1 can be activated by intracellular acidosis, mechanical pressure and depolarization. (C) TREK-1 can also act as a leak channel. This is achieved by protonation of the glutamate at position E321 or its mutation to alanine.

However, if this glutamate is protonated, the electrostatic hindrance is overcome and the proximal part of the TREK-1 C-terminus might directly interact with the intracellular layer of the membrane. This interaction was proposed to cause channel opening. It is important to notice that glutamate E321 is not only embedded in a cluster of positively charged residues, but also in a group of other titratable amino acids like D294, E309/D309 and E324. Therefore it is possible to shift the respective pK_A to about 5.5.

However, E321 is not the only residue to determine intracellular pH sensitivity. In the course of this study several new residues across the protein were shown to influence intracellular pH remarkably.

Extracellular pH-sensitivity. TREK-1 channels are also regulated by protons from the extracellular side of the membrane. Extracellular protons do not activate, but in-activate the channel (Cohen et al. 2008, Sandoz et al. 2009). Two histidine residues, H87 and H141, were singled out to effect extracellular proton inactivation, both located within the first pore loop P1 (Fig. 3). The IC_{50} for extracellular proton inactivation was pH 7.5 ± 0.2 (Cohen et al. 2008). The authors argued that a collapse of the selectivity filter caused by the additional positive charges of the protonated histidines might be the mechanistic explanation for extracellular pH gating.

Pressure sensitivity. The tension of the cell membrane is highly relevant for TREK-1 open probability: The channel is reversibly and dose-dependently activated by nega-tive pressure aka suction from the extracellular side of the cell, which results in a convex curvature of the membrane. This activation is even augmented upon disintegration of the cytoskeleton (Lauritzen et al. 2005), ruling out intracellular structures to solely mediate the channel's pressure response.

Pressure gating in TREK-1 can be mimicked by amphipathic molecules like trinitro-phenol. This exemplary anionic substance preferentially inserts into the outer layer of the lipid membrane (Patel et al. 1998b) and therefore causes a convex shape of the membrane. For this reason, trinitrophenol is also referred to as „membrane crenator" and has been shown to mimick mechanical suction in an inside-out patch. Contrarily, cationic „cup formers" like chlopromazine are able to simulate positive pressure by

inserting into the inner layer of the membrane. The phenomenon of cup-formers and crenators also suggests a possible link between mechanical and lipid regulation.

Published half maximal pressure activation values for TREK-1 vary significantly (Maingret et al. 1999, Patel et al. 1998a), as it seems extremely difficult to control all relevant variables like membrane composition and cytoskeleton integrity in order to determine universally valid figures.

Lipid regulation. From what is already known about lipid regulation in TREK-1 channels, this regulatory pathway is rather complex. While saturated lipids have no effect on the channel (Danthi et al. 2003), polyunsaturated fatty acids (PUFA) like arachidonic acid (AA) and lysophospholipids like lysophosphatidylcholine (LPC) can activate TREK-1 (Lesage et al. 2000). Interestingly, lysophospholipid activation depends on cellular integrity and therefore seems to influence channel gating in-directly, whereas PUFA are effective channel activators even in excised patches (Maingret et al. 2000a). Necessary prerequisites for PUFA activation include at least one double bond and a negative charge within the lipid molecule. Possible links between lipid and pressure activation have been observed with lysophosphatidic acid sensitizing TREK-1 to mechanical pressure (Chemin et al. 2005a).

As a third class of lipid TREK-1 activators, phospholipids like phosphatidylinositol-4,5-bisphosphate (PIP_2) that are known to influence a multitude of ion channels also affect TREK-1 gating (Chemin et al. 2005b). When they are snatched from the mem-brane by polyamines like spermine and polylysine and therefore absent from the inner leaflet of the bilayer, the activation thresholds in TREK-1 for pH and mechanical pressure were shown to be increased considerably. However, unlike other PIP_2-activated channels, TREK-1 does not exclusively depend on PIP_2. Negatively charged phospholipids might suffice to ensure TREK-1 conductance (Sandoz et al. 2011).

Furthermore, Chemin et al. described a „locked open state" of the channel in one defined experimental context: When they added phospholipids and decreased the intracellular pH, TREK-1 channels were irreversibly transformed into open leak channels, that were no longer sensitive to usual regulatory stimuli including

intracellular pH (Chemin et al. 2005b). The protocol included the following steps: Polylysine was applied first, leading to an almost silent channel due to the absence of phospholipids in the inner leaflet. Subsequently PIP_2 was added, which resulted in a recovery of channel activity. Thereupon the intracellular pH was decreased to 5.5 for a short period of time and then normalized to pH 7.2 again. As a result of this protocol, TREK-1 was no longer sensitive to internal pH alterations and its baseline activity was increased about 10-fold. However, pressure sensitivity was still present, albeit altered.

Recently, the crystal structure of a K_{ir} 2.2 channel with a bound PIP_2-derivative has been published. It helped to clarify the mechanism of PIP_2 activation in K_{ir} channels (Hansen et al. 2011): The different parts of PIP_2 interact with transmembrane and cytoplasmic domains of the channel as well as lipids within the bilayer. PIP_2 binding to the different parts of the channel forces them to come together, causing the large cytoplasmic domains to shift aside towards the transmembrane helices. This movement is hypothesized to pull open the adjacent helix bundle crossing gate. Even though this mechanism has only been demonstrated in K_{ir} channels and even though TREK-1 does not possess equally voluminous cytoplasmic domains it is most likely that the PIP_2 activation mechanism in K2P at least partly resembles that found in K_{ir} channels.

Thermal activation. TREK-1 currents can be increased by rises in temperature (Maingret et al. 2000b). As thermal activation is completely abolished upon patch excision but does not depend on the expression system it remains elusive whether or not thermosensitivity is achieved by interactions with thermosensitive partner proteins or an intrinsic thermosensitive gating mechanism of the channel.

Interaction with G-protein coupled receptors. Finally, phosphorylation by different protein kinases is important in order to link TREK-1 gating to G-Protein coupled receptors in the membrane (Bockenhauer et al. 2001, Koh et al. 2001, Murbartian et al. 2005, Fink et al. 1996). The pivotal phosphorylation sites are serine S300 for protein kinase C (PKC), S333 for protein kinase A (PKA) and S351 for protein kinase G (PKG) (Fig. 3). However, Sandoz et al. showed that with activated Gq proteins, the downstream activation of protein kinase C does not affect TREK-1 channel currents

(Sandoz et al. 2011). Neither mutations of S300, the respective phosphorylation site, nor preincubation with the PKC inhibitor calphostatin C impacted channel activity. They stated, that the effect of Gq regulation of TREK-1 channels depends specifically on the cleavage of PIP_2 into diacylglycerol (DAG) and inositol-3-phosphate (IP_3). This reasoning is based on the finding that the enzymatic cleavage of PIP_2 into phosphatidyl-4-phosphate (PI_4P) and phosphate did not cause channel inactivation.

2.4 Interdependency of channel structure and function

Mutational analyses of TREK-1 have been performed in order to clarify the role of structural motifs, single residues and entire regions of the protein. For example, the truncation of the N-terminus, TREK-1 Δ1–56, results in a channel no longer selective to potassium, but permeated by sodium ions as well (Thomas et al. 2008). Deleting the last 76 amino acids of the C-Terminus, TREK-1 ΔCt 76, converts the channel from an outward into an inward rectifier (Maingret et al. 2002).

Additionally, several residues linked to specific regulation mechanisms have been identified (Fig. 3): As mentioned above, the regulation by extracellular pH seems to rely on the protonation of two histidine residues in the first turret loop P1, H87 and H141 (Cohen et al. 2008). Secondly, intracellular pH activation in TREK-1 was hypothesized to require a glutamate in the C-Terminus of the channel, E321 (Honore et al. 2002a). Thirdly, the C-terminal tail of the channel was shown to be necessary for mechanical and lipid activation, but it is not sufficient to maintain the according gating mechanisms (Patel et al. 1998b). In this case, the C-term was found to be not a gate itself, but rather acting as a stabilizer of the open conformation of the channel (Zilberberg et al. 2000).

2.5 The channel's physiological and clinical relevance

In 2006, TREK-1-deficient rodent models were reported to resemble a „depression-resistant phenotype" (Heurteaux et al. 2006). Based on this finding, recent pharmacogenetic clinical studies linked mutations in the encoding KCNK2 gene to
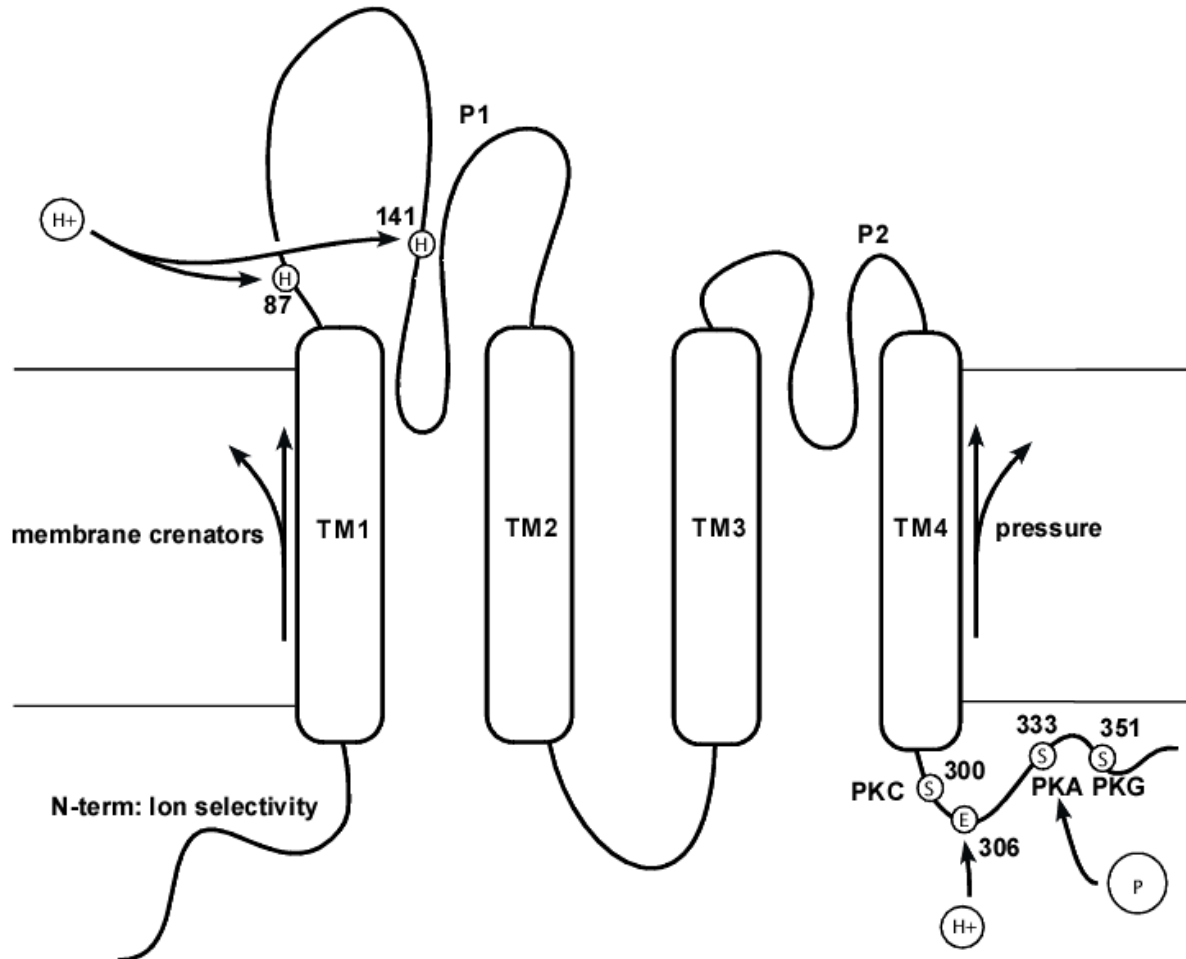

Figure 3. *Single residues linked to specific regulation pathways in TREK-1*. TREK-1 is shown with its four transmembrane helices TM1 – 4 and two pore loops (P1 and P2). Additionally, single residues that have been linked to specific regulation pathways are depicted. These include H87 and H141 regulating extracellular pH inactivation, E306 as intracellular proton sensor and the C-terminal phosphorylation sites at S300, S333 and S351. Different lengths of the N-terminus were demonstrated to change the channel's ion selectivity (Thomas et al. 2008). Convex membrane conformation and pressure increase channel open probability.

the likelihood of treatment-resistent major depressive disorder (Perlis et al. 2008). Given the high prevalence of depression and between 29% to 46% of diagnosed patients who do not respond to adequate treatment (Fava und Davidson 1996), understanding the reasons for therapy failure is essential for improving clinical results.

The clinical study „Sequenced Treatment Alternatives to Relieve Depression" (STAR*D) evaluated the importance of single-nucleotide polymorphisms (SNP) in therapy-resistant depression in a sample of 1554 patients (Perlis et al. 2008). The investigators concentrated on SNP prevalence in four genes, which had previously been shown to affect the pathophysiology of depression in rodent knockout models. Those genes included the KCNK2 gene, which encodes TREK-1, SLC18A2, a monoamine VMAT2 transporter, HDAC5, a histone deacetylase and S100A10, which encodes p11, a protein responsible for 5-HT$_{1B}$–receptor modulation.

Screening patient samples for SNP in all these candidate genes, only four SNP in the KCNK2 gene were strongly correlated with treatment-resistant depression. SLC18A2, HDAC5 and S100A10 did not display any significant associations. To assess the importance of KCNK2 genetic variations in healthy humans rather than a population of patients, further functional MRI (fMRI) studies focussed on KCNK2's impact on reward processing (Dillon et al. 2010). Significant associations were detected between the number of healthy KCNK2 alleles and responses to gain, i.e. money, by basal ganglia, regions of the frontal cortex and the dorsal anterior cingulate cortex.

Besides its importance for rewarding processes and the pathophysiology of depression, studies on TREK-1-knockout mice identified possible additional physiological functions of the channel, such as sensitivity for anesthetics, the vulnerability to ischemia and epilepsy as well as thresholds in thermal and mechanical nociception (Heurteaux et al. 2004, Alloui et al. 2006).

The latter was proposed to be mainly achieved by the TREK-1 channel acting as a molecular counterpart of the colocalized TRPV1 channel: TRPV1 is considered a „key molecule" in peripheral pain sensation. Expressed in nociceptive neurons, this

non-selective cation channel causes depolarization when activated by stimuli like pH, heat, capsaicin and PIP_2 (Tominaga und Tominaga 2005). TREK-1, also activated by the majority of these stimuli with the exception of capsaicin, could reverse the depolarizing effect of TRPV1 by allowing K^+ outflow, therefore acting as a molecular counterpart of TRPV1. Intriguingly, TREK-1 and TRPV1 show extensive colocalization in sensory neurons (Alloui et al. 2006, Yamamoto et al. 2009). Moreover, TREK-1 knockout mice display increased thermal and mechanical sensitivity, especially within the thermal interval between 40 and 45°C (Alloui et al. 2006). Thus, the threshold of nociceptive neurons might be regulated by balancing TRPV1 and TREK-1 expression in the peripheral nervous system, hence modulating the extent of pain perception.

Additionally, possible roles of TREK-1 in bladder excitability and myometrial quiescence have been argued (Bai et al. 2005, Baker et al. 2008, Buxton et al. 2010). Unlike previously reported, the lack of TREK-1 in rodent models seems to have no effect on vasodilation (Namiranian et al. 2010).

2.6 Gating Modes in classical K^+ channels

Three distinct gating mechanism have been proposed to enact channel gating in classical potassium channels – C-type, N-type and so-called „helix bundle crossing" (BC) gating. It is usually assumed that these gating modes resemble canonical patterns for the majority of K^+ channel families. However, it remains elusive if they can fully explain gating in K2P channels.

N-terminal inactivation gate. N-type gating in K^+ channels was prototypically described for the *Shaker* K^+ channel. In this and other voltage-dependent K^+ channels, fast inactivation is achieved by a small N-terminal „ball" protein domain usually comprising the first 20 amino acids of the channel subunit. This ball peptide is flexibly connected to a protein linker that attaches it to the first transmembrane helix. It can block the channel by entering and occluding its cavity. As no ball peptide is present in K2P channels, N-type inactivation possesses no relevance in K2P channels.

C-type gating. The concept of C-type gating is currently based on the idea that conformational changes within the selectivity filter can lead to its destabilization, therefore obviating ion conductance. „C-type inactivation" was first described in the early 1990s, when voltage-dependent K^+ channels without the N-terminal ball domain were studied. It was noted that, in the absence of the N-terminal ball domain, channels would still inactivate, albeit slowlier. Furthermore, wild-type channels with intact ball peptide showed a two-exponential time course of channel inactivation. This phenomenon could only be explained by two different inactivation mechanisms (Choi et al. 1991): Fast inactivation was correctly identified as N-type inactivation whereas the slower inactivation process remained elusive. Following studies showed the latter's dependence on the permeant ion, extracellular ion concentrations and blocking molecules. The underlying mechanism was soon described as „C-type inactivation", a term coined in contrast to „N-type" gating (Hoshi et al. 1991).

To understand the mechanisms behind C-type gating, it is necessary to understand ion conduction through the channel. A potassium channel's pore is made up of three different parts – the channel cavity opening towards the intracellular space, the narrow filter located in the outer third of the membrane and an extracellular part where the C-terminal ends of the alpha helices come together with their negative end charges and stabilize one extracellular K^+ ion. The channel cavity is about ten Ångström in diameter, giving space to a potassium ion that is fully hydrated with six water molecules. Hydrating the ion until it has entered the centre of the the pore and therefore halfway through the membrane lowers the necessary energy for the ion to traverse this part of its way through the energy barrier between intra- and extracellular areas. However, the cavity cannot secure selectivity, which must be achieved by the adjacent filter region.

The selectivity filter is the central and best conserved domain in all ion channels. A canonical sequence of TTXG Y/F G forms a loop that reaches into the channel cavity. Together with the three loop counterparts of the other subunits in tetrameric channels, it narrows the pore's outer third, creating a small filter path with four potassium binding sites (Fig. 4). This path is too narrow for a fully hydrated potassium ion to pass. However, if the ion is dehydrated with only two or three water molecules left at its side, it fits the selectivity filter region, which structurally mimicks

the ion's hydration shell: Eight backbone oxygen atoms are coordinating the ion in every single of the four central filter binding sites in a way reminiscent of the H_2O shell. Additionally, three peripheral K^+ binding sites exist, S0 on the extracellular side, S5 on the intracellular side and S6 in the channel cavity. Whereas ions like rubidium, caesium and thallium can pass this selectivity filter, sodium ions cannot. The underlying selectivity is mainly achieved by a combination of a higher dehydration energy for sodium ions and steric reasons, as the Na^+ ion is smaller in size than the K^+ ion, leading to a fail of the backbone oxygens atoms to cordinate a sodium ion.
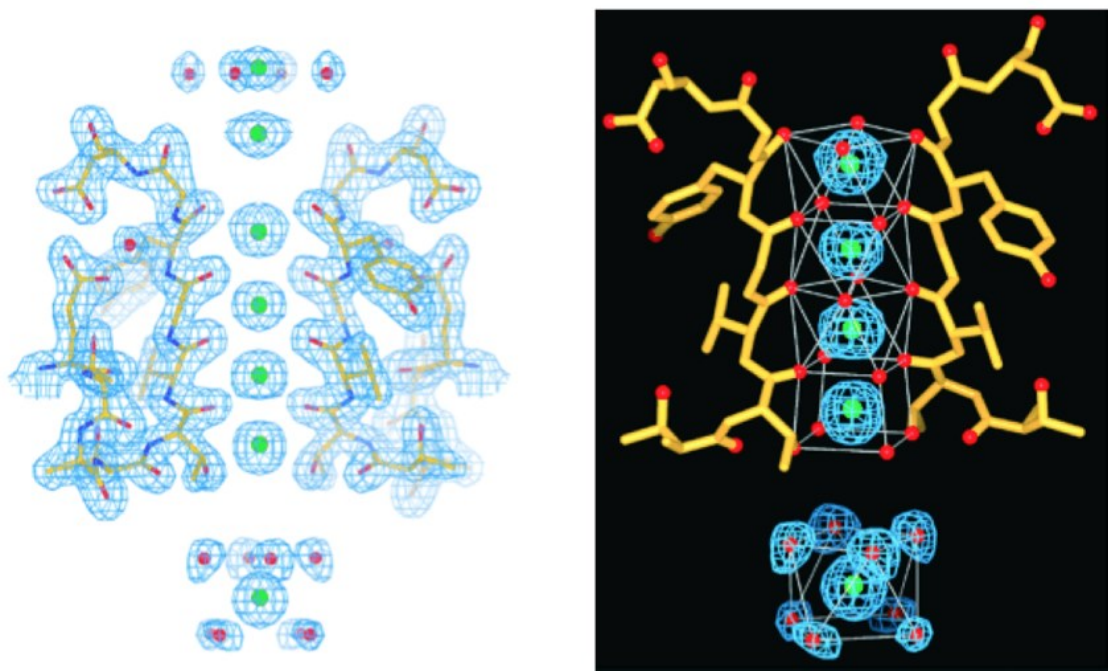

Figure 4. *The selectivity filter region of classical potassium channel with the canonical K^+ ion binding sites (MacKinnon 2004)*. Depicted are prototypical structures of a K^+ selectivity filter based on a *KcsA* high-resolution structure. The transmembrane helices are hidden out in this illustration. Four K^+ binding sites, S1 – 4, can be seen within the selectivity filter. Backbone oxygens are depicted red, including those that coordinate K^+ ions. Below S1 – 4, a fully hydrated K^+ ion is shown located within the channel cavity. On the left panel, the additional putative binding sites for a sixth and seventh K^+ ion are shown on the extracellular side.

The filter structures in Na^+ channels are slightly wider, but their exact mechanism of selectivity has not been identified yet. However, the concept of a fixed filter diameter as central feature for ion selectivity has been called into question. In molecular simulations of K^+ flux in the *KcsA* filter, the positions of carbonyl oxygens were shown

to be quite variable (Berneche und Roux 2001), ruling out a bigger role of the filter diameter and instead stressing the importance of higher energetic barriers for Na^+ ions crossing the filter gate. Given the sophisticated requirements for K^+ conduction, it seems clear that even small conformational alterations in this region can obviate the entire ion flux. Over the past two decades, evidence for a filter-related mechanism for C-type gating in K_v channels and mechanisms reminiscent of C-type gating in other K^+ channels has accumulated. Exemplarily, a possible mechanism was demonstrated in the prokaryotic inward-rectifying *KcsA* channel (Cordero-Morales et al. 2006): Upon the introduction of E71A, only three residues upstream of the selectivity filter motif in *KcsA*, the open probability (P_o) increases dramatically from ≤ 0.2 to ~ 0.95-0.99. Additionally, the crystallized E71A mutant shows remarkable conformational alterations within and close to the filter region. In one of the two detected, crystallized states, the mutation caused a reorientation of the filter motifs' backbones most likely due to the disrupted carboxyl-carboxylate interaction between a glutamate and an aspartate at positions E71 and D80. Even more recently, *KcsA* was crystallized in a set of different conformations, not only showing different stages of helix bundle opening but also the supposed intermediate states of the selectivity filter (Cuello et al. 2010a).

Helix bundle gating. Whereas C-type gating seals off the K^+ permeation pathway within the selectivity filter, a second gating region exists in K_v and K_{ir} channels. This gate regulates the channel entrance on the intracellular side. The so-called helix bundle crossing or BC gate is currently understood as a narrowing of the inner third of the channel directly below the channel cavity. It is formed by the four inner helices (M2 in K_{ir} channels, S6 in K_v channels and theoretically M2/M4 in K2P channels). These helices traverse the membrane at an angle of about 25° and converge on the intracellular side of the membrane (Doyle et al. 1998). The resulting narrowing of the interhelical diameter in this region is described as bundle crossing (BC) point (Labro und Snyders 2012).

In order to enable opening and closure, the diameter of the BC point must be flexible. With the K^+ ion's diameter of about 2.66 Ångström, reducing the BC diameter to 2.0 Ångström would be sufficient to hinder K^+ ions from entering the channel cavity. However, it has been argued that an opening as wide as six Ångström would be

sufficient to obviate ion and water permeation if the opening was lined by hydophobic residues (Beckstein et al. 2004). On the other hand, big TEA derivatives have been shown to be able to enter and stay within the central cavity (Zhou et al. 2001), implying that the BC gate can open as widely as eight to ten Ångström.

Different mechanisms have been proposed to explain the transition between these open and closed BC conformations based on studies in other K^+ channel families, especially the *Shaker* K_v channel. The currently emerging consensus explains BC gating as a movement of the inner helices, tilting away from the central axis and thereby opening the channel entrance like the aperture of a camera (Labro und Snyders 2012). So far, two slightly different models for this movement have been proposed for the different K^+ channel families: In classical voltage-gated K^+ channels with six transmembrane helices in one subunit like *Shaker*, the pore-lining helix S6 contains two „hinge" motifs to allow for gating: Firstly, a conserved glycine residue is positioned 20 residues downstream the GYG selectivity filter motif. Secondly, seven residues after this glycine, a PVP (proline-valine-proline) motif is located roughly halfway through the membrane. Given these two flexible hinge motifs, the S6 helix is thought to kink at the PVP motif, thereby opening the channel entrance in voltage gated K^+ channels (del Camino et al. 2000). In contrast, no PVP motif exists in K^+ channels with only two transmembrane helices per subunit (2TM-1P), e.g. *Kcsa* or *MthK*. However, they still contain the conserved glycine 20 residues downstream the filter motif and are thought to open their BC gate by bending their M2 helix outwardly, using this conserved glycine as a hinge (Labro und Snyders 2012).

2.7 Currently known blockers of TREK-1

For a long time after their discovery, functional studies on K2P channels remained very difficult due to a lack of inhibitors. All classical potassium channel blockers like tetraethylammonium (TEA), 4-aminopyridine (4-AP) and Cs^+ failed to block K2P channels when applied from the extracellular side (Fink et al. 1996, Fink et al. 1998). However, since then many molecules blocking TREK-1 currents have been identified (Table 2), among them the classical calcium channel blocker amlodipine (Liu et al. 2007), antidepressants like fluoxetine (Kennard et al. 2005), antipsychotics (Thümmler et al. 2007) and the amino acid methionine (Mongahan et al. 2011). As results are based on different types of electrophysiological recordings and expression systems, published IC_{50} are hardly comparable.

Table 2. *Currently known inhibitors and activators of TREK-1 channels.* The respective first publication reporting an effect on the TREK-1 channel is stated in the second column.

Blockers	
Amlodipine, Niguldipine	(Liu et al. 2007)
Antipsychotics Fluphenazine, Chlorpromazine, Haloperidol, Flupenthixol, Loxapine, Pimozide	(Thümmler et al. 2007)
Cisplatin	(Milosavljevic et al. 2010)
Curcumin	(Enyeart et al. 2008)
Fluoxetine, Norfluoxetine	(Kennard et al. 2005)
Lidocaine	(Nayak et al. 2009)
Maprotiline	(Eckert et al. 2011)
Methionine	(Mongahan et al. 2011)
N-6-substituted cAMP-analogs	(Liu et al. 2009)
N-Butylphalide	(Ji et al. 2011)
Quinidine	(Patel et al. 1998b, Zhou et al. 2009)
Spadin	(Mazella et al. 2010)
TEA-derivatives	this study
Tri-/Tetracyclic antidepressants: Citalopram, Mirtazapine, Doxepine	(Eckert et al. 2011)
Zinc	(Gruss et al. 2004)
Activators	
Anesthetics Chloroform, Diethyl ether, Halothane, Isoflurane	(Patel et al. 1999)
Copper	(Gruss et al. 2004)
Trichlorethanol	(Harinath und Sikdar 2004)
Riluzole	(Duprat et al. 2000)

2.8 The TnA-blocker family

Tetraethylammonium (TEA) and its derivatives (TnA), also known as quaternary ammonium compounds (QA), are long-known pore blockers of classical potassium channels (Armstrong 1966). Consisting of a central nitrogen atom and four bound n-alkyl tails, they act as open channel blockers in K_v and K_{ir} channels, meaning that the channel has to open before the TnA molecule can enter the channel pore and occlude it. Consequentially, they can support studies on channel gating mechanisms, especially enlightening the role of channel gates at the intra- or extracellular entrance of the channel. Additionally, they provide insight into the cross section of the molecule in different parts of the permeation pathway as well as its length (Miller 1982). In classical potassium channels, increasing the length of one or more n-alkyl tails also enhances affinity for intracellular TnA block (Armstrong 1971). Not least because of missing open channel pore blockers for K2P channels, the gating mechanism of channels like TREK-1 has not been studied in detail. Before the present study, TEA had always been reported to be unable to block TREK-1 channels from the extracellular side (Fink et al. 1996, Fink et al. 1998). In one single study focussing on the K2P channel TASK-2, the sensitivity of a K2P member towards cytosolic TEA was demonstrated (Cotten et al. 2004). TEA derivatives with longer alkylic side chains like Tetrapentylammonium had not been studied in K2P channels.

3 Aim of this study

Despite their assumed physiological relevance and possible role in pharmacology, the pore structure and gating mechanisms of K2P channels are only poorly understood. As K2P architecture differs markedly from all previously studied potassium channels it remains unclear whether K2P channels actually employ the same gating principles as classical potassium channels. In order to study gating, it is helpful to identify pore blockers. These molecules have to pass cytosolic channel gates and subsequently enter their binding site in the channel cavity. They enable studies regarding pore diameter, gating movements and constriction regions. Furthermore, they can identify pore lining residues, thus enabling validation of in-silico models and crystal structures. Even though several inhibitors of the TREK-1 channel are known, their binding site, let alone blocking mechanisms have not been identified.

Consequentially, the first aim of this study was to retrieve and characterize pore blockers for TREK-1. Therefore, a cysteine scan of pore-lining residues was employed to identify the TPenA blocker binding site. Furthermore, the dependence of blocker affinity on open probability, extracellular potassium concentration and different permeating ions was tested. On the basis of those results, conclusions could be drawn regarding the channel pore's structure, likely conformational changes during the gating process and the location of the channel gate itself.

4 Methods

Mutagenesis, cRNA synthesis and injection in Xenopus laevis oocytes. Studies were performed using the rTREK-1 channel (NM_172042), the TASK channel, the TRESK channel, the K_{ir} 1.1 channel and the modified Δ6-46 *Shaker* channel, which lacks the N-terminal ball peptide. Mutations in TREK-1 were introduced by site directed mutagenesis (QuikChange II, Stratagene, La Jolla CA, USA), followed by sequence verification. Constructs were subcloned in pGEM and pBF vectors. mRNA synthesis was achieved using SP6 mMessage mMachine, Ambion, Austin TX, USA, prepared by Dr. H. Fritzenschaft in the Baukrowitz laboratory and L. Shang in the Tucker group. mRNA was stored at -80°C.

Surgical oocyte preparation of Dumont stage VI oocytes was performed on female *Xenopus laevis* frogs at four-weekly intervals. Oocyte treatment included manual dissection after collagenase conditioning, using 0.5 mg/dl collagenase II (Sigma, Taufkirchen, Germany). Oocytes were then stored in Barth's solution. Between eight to 36 hours after preparation, mRNA solution was injected and injected oocytes were incubated in Barth's Solution at 19°C for twelve hours to seven days, and defolliculated on the day of the electrophysiological measurement.

Electrophysiological measurements. Data were obtained measuring giant inside out patches in voltage clamp conditions. Pipettes from thick walled borosilicate glass had a resistance ∈ [0.15; 1] MΩ. They were filled with a solution containing 120 mM KCl, 10 HEPES and 1,8 $CaCl_2$. If required, pH was adjusted to 7.2 using KOH. For low external potassium concentrations, this solution was modified to 4 mM KOH, 116 mM NaOH, 10 HEPES and 1.8 $CaCl_2$. Intracellular solutions were applied using a multibarrel pipette made from double barrel theta glass capillaries. Intracellular solutions contained 120 mM KCl, 10 HEPES, 2 mM EGTA and 1 mM $NaPP_i$. This solution was adjusted to the required pH using HCl and KOH, respectively.

Tetraethylammonium derivatives (TnA), including Tetraethylammonium chloride (TEA), Tetrabutylammonium bromide (TBA), Tetrapentylammonium chloride

(TPenA), Tetrahexylammonium chloride (THexA), Tetraheptylammonium bromide (THepA) and Tetraoctylammonium chloride (TOA) were purchased from Sigma. Substances were stored as stock solutions ranging from 10 to 100 mM at -20°C.

Currents were measured using an EPC10 amplifier (HEKA electronics, Lamprecht, Germany) and a chlorided silver wire inside the pipette. An additional bathing electrode was employed to serve as a reference electrode. Currents were sampled at 10 kHz and filtered at 3 kHz. Pressure was applied by the HSPC 1 device (Ala Scientific Instruments, Famingdale NY, USA). Unless otherwise stated, currents were recorded at – 80 mV in symmetrical potassium concentrations.

Data analysis. Data were analyzed using Igor Pro 4.09A Software (Wavemetrics Inc., USA). Graphing was performed with Canvas 8 (Deneba Systems, USA), statistical analysis with Microsoft Excel 2008 (Microsoft, USA). Relative steady state levels for different blocking compounds including TnA blockers and pH were fitted based on the Hill equation. IC_{50} measurements for TPenA in TREK-1 WT and mutants were compared by paired samples t-test. The null hypothesis was rejected at $P < 0.05$.

Illustrations. Channel representations were created using VMD, Multiple Alignment Plugin, Interactive Molecular Dynamics (IMD), Tachyon (Humphrey et al. 1996) employing preliminary *KvaP*-derived TREK-1 models provided by the Sansom group in Oxford.

5 Results

5.1 TnA derivatives are high-affinity blockers in TREK-1

Previous to this study, different groups had published data demonstrating that TREK–1 channels are insensitive towards extracellular tetraethylammonium (TEA) at concentrations that are sufficient for channel block in K_{ir} and K_v channels (Fink et al. 1996, Fink et al. 1998). The effect of higher intracellular TEA concentrations or TEA derivatives (TnA) had not been explored in detail. In our initial experiments, only very high concentrations of intracellular TEA resulted in partial TREK-1 blockage (Fig. 5).

In 1971, Clay Armstrong showed that increasing the hydrophobicity of TnA side chains boosts the affinity of TnA blockers applied from the cytosolic side (Armstrong 1971). He worked with TEA derivatives in which only one side chain was altered: He replaced one ethyl group with either unbranched hydrocarbon side chains or carbon linkers that attached a benzene ring to the quaternary nitrogen. He demonstrated that blocker affinity increases with longer side chains in all those TEA derivatives. This being the case, it was hypothesized at the beginning of the present study that TREK-1 resilience towards cytosolic TEA block could be overcome by increasing the length of carbon chains, resulting in higher hydrophobicity. As TEA derivatives with only one altered side chain were not commercially available, it was decided to employ symmetrical variants. In those, every central nitrogen is accompanied by four un-branched carbon chains of equal length. I tested molecules with alkyl-chain lengths ranging from four to eight carbon atoms by comparing blocker affinity for these molecules in TREK-1 channels. Inside out giant patches with the intracellular side of the membrane facing the bath solution were exposed to increasing blocker concentrations, resulting in dose-response curves of inhibition with at least four different concentrations of the blocking molecule in each experiment.

Before each experiment the patch was exposed to two different pH solutions at pH 5.5 and 8.0. As TREK-1 is closed in the presence of pH 8.0 unless additional stimuli like positive pressure are applied, the remaining current at pH 8.0 was considered to
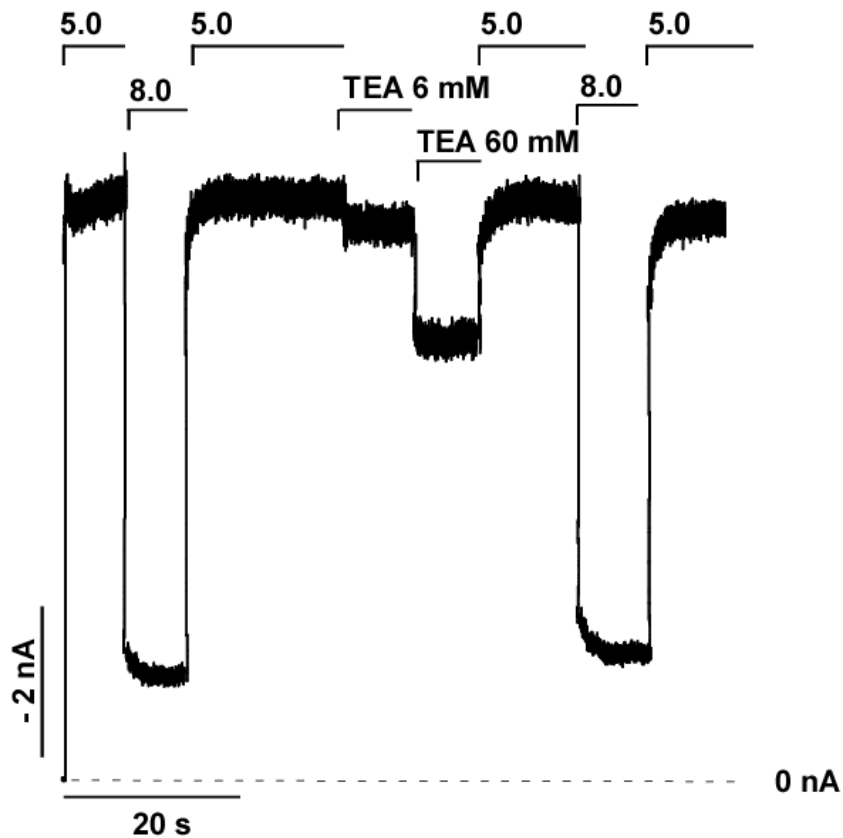
Figure 5. *Intracellular TEA shows almost no inhibitory effect on TREK-1*. When applied from the intracellular side in the presence of pH_{ic} 5.0, even high concentrations of TEA only block a minor fraction of TREK-1 channels. Channel inactivation by intracellular pH 8.0 is shown as a control.

resemble potassium conductance distinct from TREK-1 currents and was therefore substracted from the measured current at pH_{ic} 5.5, resulting in I_{max}.

$$I_{max} = I_{pH5.5} - I_{pH8.0}$$

In a fraction of patches, an initial „run-up" of current was observed, most likely reflecting a change in membrane lipid composition due to patch excision (Schmidt und MacKinnon 2008). In these cases, experiments were started after $I_{pH5.5}$ had been stable for more than 10 seconds. To rule out further additional stimuli like temperature and positive pressure, all solutions were applied at room temperature ranging from 19 to 25°C. Before conducting the blocker experiments, the multibarrel application system was tested with plain pH 5.5 solution in all of its chambers to rule out differences in flow pressure between the different application slots. In this

experiment, no impact of the different slots of the application system on patch current was detected.

TnA dose response curves were obtained in giant patches with at least four different concentrations of the respective substance applied (Fig. 6). The extent of block was determined expressing the remaining current I as a fraction of maximum current I_{max}. Subsequently, I/I_{max} was plotted against blocker concentration. The resulting plots were fitted to the Hill equation:

$$I/I_{max} = (([TnA]/IC_{50})^n + 1))^{-1},$$

[TnA] representing blocker concentration, n representing the Hill coefficient, I representing the respective current, I_{max} representing the maximum current and IC_{50} referring to the blocker concentration at which half-maximum inhibition was achieved. Tetraethylammonium (TEA) showed almost no inhibitory effect on TREK-1 with an estimated IC_{50} of 60 mM in accordance with previous reports (Fig. 5).

Blocker affinity then increased sharply for larger TEA derivatives: The IC_{50} decreased from 2 ± 0.3 mM in Tetrabutylammonium (TButA), to 13 ± 2 µM in Tetrapentyl-ammonium (TPenA) and to 1 ± 0.4 µM in Tetrahexylammonium (THexA, see Fig. 6). Due to a slow second component of inhibition, the IC_{50} of Tetraheptylammonium (THepA) and Tetraoctylammonium (TOA) could not be determined for TREK-1, but could be measured in the more TnA-sensitive K2P members TRESK and TASK-3 by my colleague Dr. M. Rapedius.

To further characterize the biophysical properties of TnA block, I examined the voltage dependency in TREK-1 channels. TREK-1, unlike K_{ir} channels, showed only mild voltage dependence of TnA block. Upon a 160 mV voltage shift, current block increased only by ten percent closely resembling voltage-independent TnA block in K_v channels (Fig. 7).
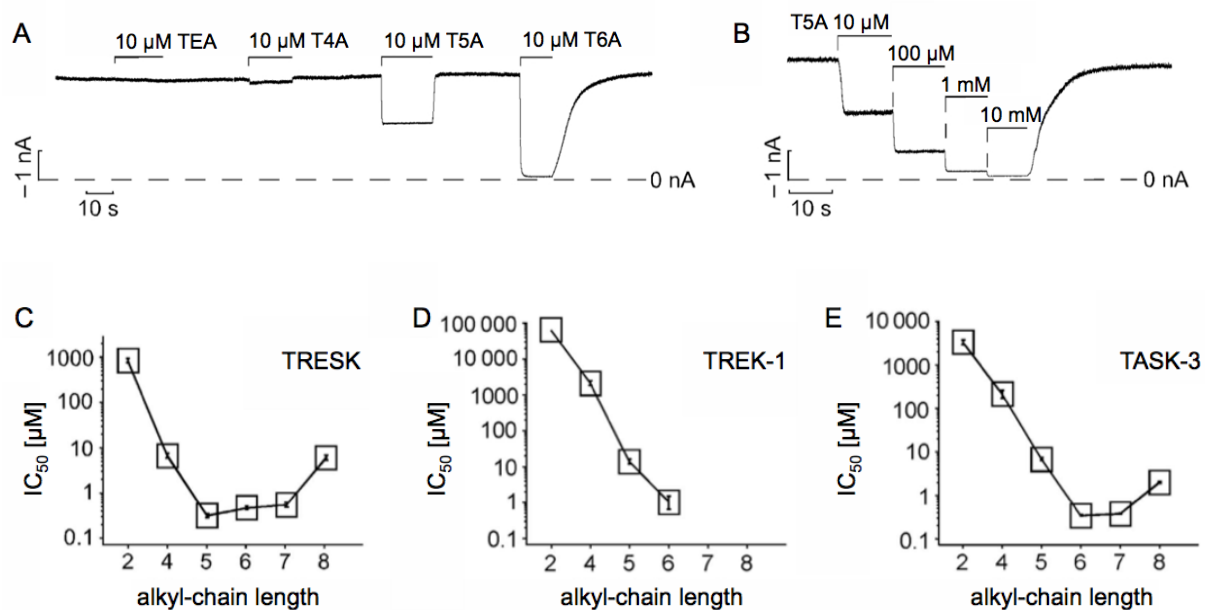
Figure 6. *TnA molecules block TREK-1 from the intracellular side*. (A) When applied from the intracellular side, blocker affinity of TnA increases with increasing chain length. (B) An exemplary dose response measurement in TREK-1 with four different concentrations of TPenA applied. After blocker removal, full recovery of the current is observed. (C-E) IC_{50} values of TnA compounds depending on the length of the hydrophobic side chains. In TREK–1, IC_{50} values for THepA and TOA could not be determined due to a reproducible, pronounced and slow second component of block, whose cause remains unknown. Experiments for TRESK and TASK-3 channels were performed by Dr. M. Rapedius.

5.2 Identifying the TnA blocker binding site

In order to identify the T5A binding site in TREK-1 channels, a cysteine scan of both transmembrane helices TM2 and TM4, the pore regions P1 and P2 as well as an additional stretch of amino acids in the proximal C-terminal region was employed. These regions were selected on the basis of a previously derived, unpublished *KcsA* homology model of TREK-1 proposed by Prof. Sansom's group in Oxford. That model predicted these residues to represent the pore-lining regions. Mutants were prepared by Dr. H. Fritzenschaft in the Baukrowitz group and L. Shang in the Tucker
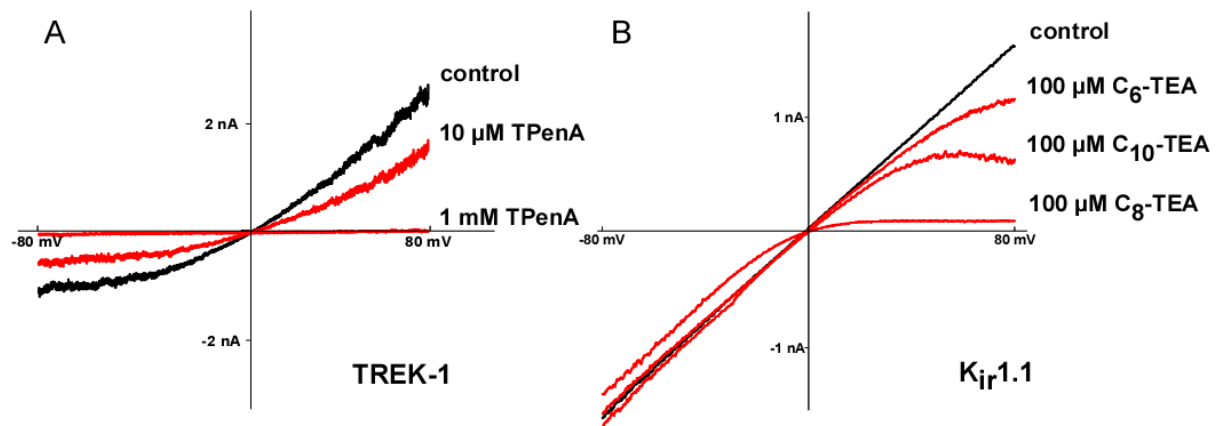
Figure 7. *TnA blockage in TREK-1 is voltage-independent.* (A) Exemplary voltage ramps with pulses from - 80 to + 80 mV are shown in the presence of pH_{ic} 5.0 and different concentrations of tetrapentylammonium (TPenA) for TREK-1 as a member of the K2P family. Block by TpenA shows only subtle voltage-dependence. (B) Exemplary voltage ramps with pulses from - 80 to + 80 mV are shown in the presence of pH_{ic} 7.2 for K_{ir} 1.1. The chanel is blocked voltage-dependently by different TEA-derivatives with a single alkyl side chain, namely C_6-TEA, C_8-TEA and C_9-TEA.

lab. Altogether, 49 cysteine TREK-1 mutants were included: I155C to I158C in the first pore loop, I182C to G201C forming the second transmembrane helix, L264C to I267C in the second pore loop, I293C to W310C in the fourth transmembrane helix and L311C to K316C as a proximal part of the C-terminus (Fig. 8).

None of these residues was a cysteine in the wild-type. We assumed, that introduced cysteines would not form additional disulfide bridges and would not profoundly alter the structure of the channel cavity or possible binding sites. Only one mutation (G296C) within the scanned regions resulted in a non-conducting channel. The comparatively large proportion of functioning mutants might be explicable by K2P's special architecture: Because of its dimeric structure, a cysteine scan in TREK-1 only introduces two altered amino acids into the protein. In tetrameric channels like K_{ir}, mutagenesis results in four altered sites per channel protein. This less significant perturbation of the channel in dimeric K2P channels might explain a lesser risk of non-functional proteins.
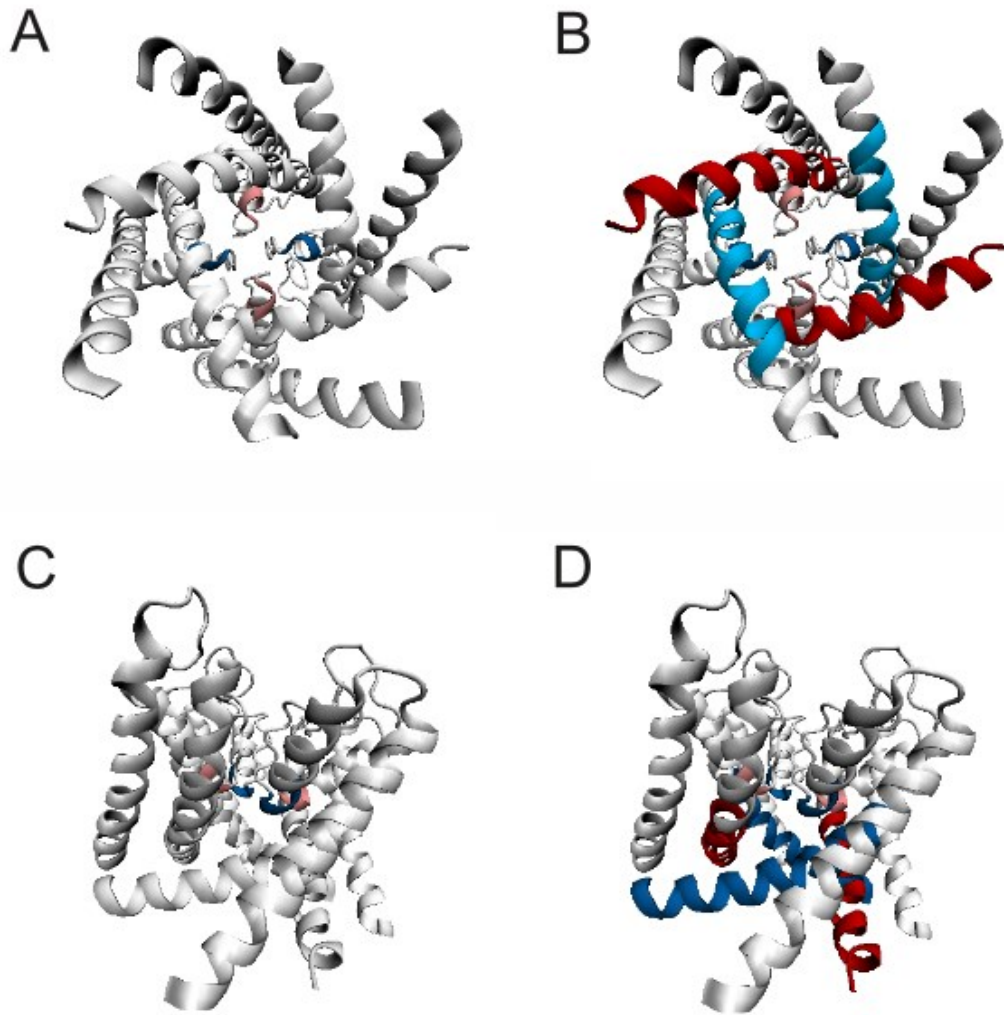
Figure 8. *Cysteine scan of pore lining residues in TREK-1: Scanned regions in pore and inner transmembrane regions.* (A) Mutated residues I155 to T157 (red) in P1 and L264 to T266 (blue) in P2 shown in a bottom-up view of TREK-1 in a *KvaP*-based model. (B) Scanned residues in both inner transmembrane helices TM2 (red) and TM4 including four C-term residues (blue) along with the pore mutants shown in a bottom-up view of the channel. (C) Mutated residues I155 to T157 (red) in P1 and L264 to T266 (blue) in P2 shown in a side view of TREK-1 in a *KvaP*-based model. (D) Scanned residues in both inner transmembrane helices TM2 (red) and TM4 including four C-term residues (blue) along with the pore mutants shown in a side view. Channel illustrations were created in VMD and are based on a *KvaP*-derived model provided by the Sansom group in Oxford.

For all these mutants, TPenA IC_{50} was measured. Although a number of IC_{50} alterations were detected, only alterations bigger than a three-fold increase were

considered to be functionally significant. As a result, twelve residues were identified that shifted TPenA IC$_{50}$ of wild-type channels considerably (Table 3, Fig. 9). These residues included T157C in P1; I182C, P183C and L189C in M2; T266C in P2 and G296C, A298C, Y299C, L304C, S305C, I307C and D309C in M4.

Not all residues in the cysteine scan that reduced or increased blocker affinity are likely to directly interact with the TPenA molecule. P183C might change blocker affinity because of its profound effect on transmembrane helix conformation and proximity to I182 rather than being part of the binding site. This rationale can be applied to all detected mutations which are located next to each other, as I182/P183, A298/Y299 and L304/S305 are positioned within α-helix regions and therefore only one residue of each pair can face the inner cavity in the absence of conformational changes. Therefore, we differentiated between those residues that directly interact with TPenA and those which might only indirectly influence TPenA binding. Additionally, the plausibility of the putative binding site was tested in several MD simulations by the Sansom group in Oxford. In those simulations, 18 different homology models of TREK-1 were evaluated. Both closed and open state homology models were included: Closed state templates ranged from crystal structures of *MlotiK* and NaK, open state models included several *KcsA* structures as well as *KvAP*, *MthK*, Kv1.2 and NaK. Furthermore, two recently published TREK-1 models were included (Treptow und Klein 2010, Milac et al. 2011). Consequently, the twelve residues that markedly altered TPenA affinity in our experiments were evaluated for interactions with an optimally docked TPenA molecule.

As a result, the combined evaluation of structural plausibility and MD simulations led to the differentiation of the twelve candidate residues, that is represented in Fig. 8: Those residues likely to form the blocker binding site are coloured in emerald green, namely T157, I182, L189, T266 and L304. Those which supposedly shift TPenA affinity solely by indirect interactions with the blocker molecule are depicted in light green.

Table 3. *Alterations in TPenA IC_{50} in a cysteine scan of pore lining residues in TREK-1.* Values are given for each mutation as well as the double mutant TREK-1 T157C-L189C. Residues that shifted the mean IC_{50} more than three-fold are highlighted in red. *P < 0.05.

| mutant	n	IC_{50}		SD	SEM	mutant	n	IC_{50}		SD	SEM
WT	10	14		4.1	1.3	266	5	102	*	20.6	9.2
155	7	27	*	5.1	1.9	267	4	14		2.0	1.0
156	4	11		2.4	1.2	293	11	22		10.0	3.0
157	5	123	*	25.5	11.4	294	5	10		2.4	1.1
158	3	6	*	1.1	0.7	295	3	16		6.5	3.8
182	8	121	*	41.7	14.8	296	5	81	*	39.2	17.5
183	7	60	*	21.0	7.9	297	7	5	*	0.9	0.3
184	3	19		16.5	9.5	298	10	59	*	16.4	5.2
185	3	16	*	2.9	1.7	299	6	53	*	16.7	6.8
186	3	6	*	1.9	1.1	300	3	11		3.5	2.0
187	4	21		12.7	6.4	301	3	16	*	1.2	0.7
188	4	25		34.1	17.1	302	4	30	*	3.0	1.5
189	6	120	*	43.1	17.6	303	3	32		9.6	5.5
190	3	13		4.2	2.4	304	10	64	*	19.1	6.0
191	4	36		19.4	9.7	305	8	73	*	22.0	7.8
193	4	19	*	1.7	0.9	306	6	31	*	11.6	4.7
194	9	32	*	10.8	3.6	307	12	73	*	30.9	8.9
195	4	21	*	4.3	2.2	308	3	33	*	6.8	3.9
196	6	28	*	2.2	0.9	309	6	52	*	13.5	5.5
197	7	29	*	11.1	4.2	310	5	22		10.6	4.7
198	5	9		1.4	0.6	311	6	35	*	7.8	3.2
199	4	10		2.3	1.1	312	4	10		1.7	0.9
200	3	14		5.5	3.2	313	3	17	*	2.6	1.5
201	6	17		6.3	2.6	316	3	23		4.4	2.5
264	10	23		16.3	5.1	T157C-L189C	4	4390	*	2708.1	1354.1
265	3	12		1.2	0.7						
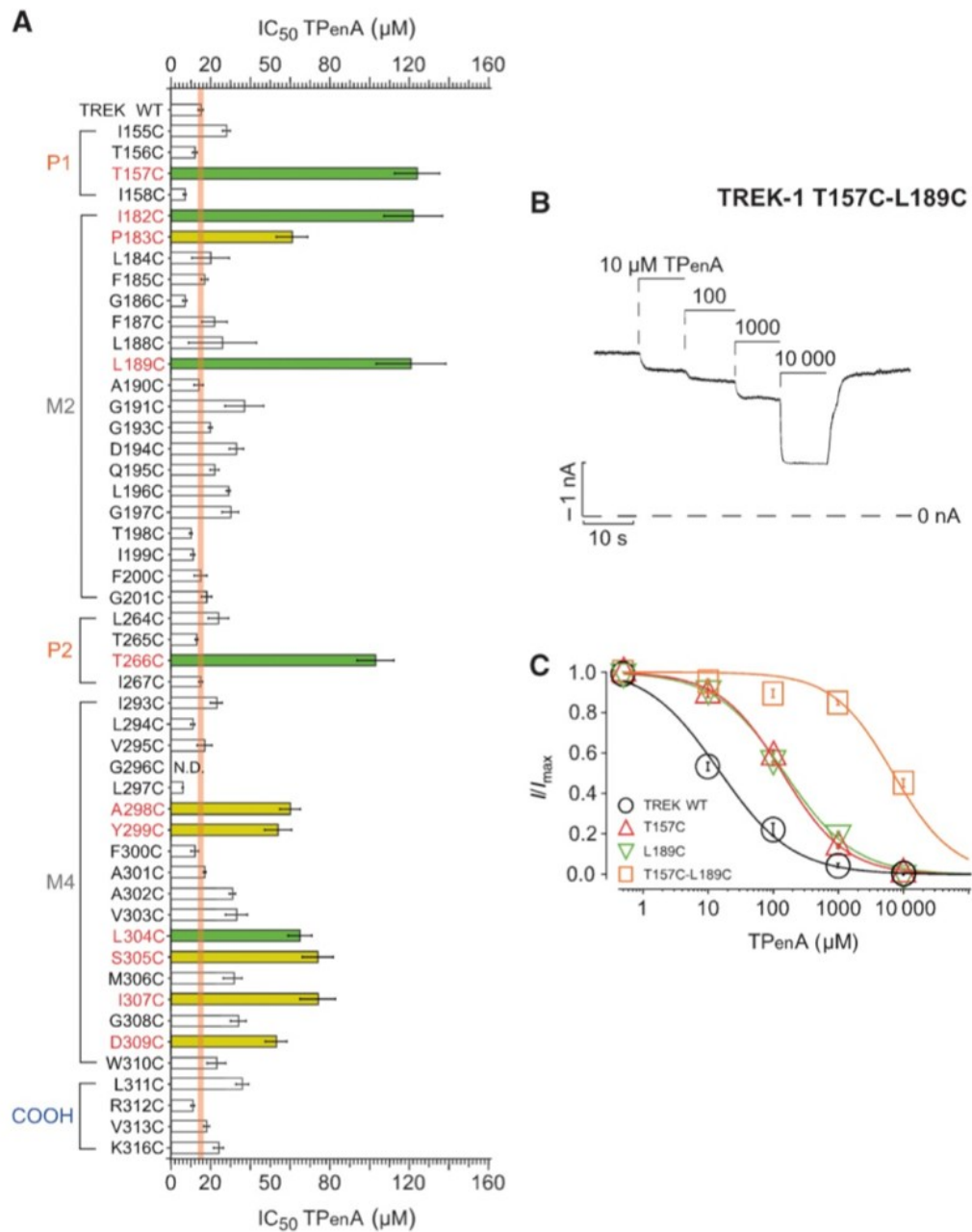
Figure 9. *Identification of the TPenA binding site in TREK-1.* (A) Cysteine scan of pore lining residues in TM2 and TM4, the pore regions P1 and P2 as well as four C-terminal residues („COOH") and respective TpenA IC_{50} values. The vertical red line represents the corridor of the TPenA IC_{50} standard error of the mean in TREK-1 wild-type. Directly interacting residues are highlighted in emerald green, indirectly interacting residues are depicted in light green. (B) Exemplary TPenA dose response trace of the T157C-L189C double mutant in TREK-1, which is not fully inhibited by 10 mM TPenA. (C) TPenA affinity fitted with a standard Hill equation for TREK-1 WT, the mutants T157C, L189C and T157C-L189C.

However, even the largest detected shifts in TPenA affinity upon cysteine introduction were rather mild. Comparable mutational analyses in other K_{ir} channels showed up to 100-fold changes in TEA affinity caused by a single alanine mutant within the channel cavity (Shin et al. 2005). As mentioned before, this might somehow be explainable by the dimeric structure of K2P channels: As the entire channel protein is formed by only two subunits, introducing a mutation results in only two altered amino acids in the whole channel protein. Contrarily, in tetrameric channels, one mutation would cause four amino acids within the channel to be changed. Even though this might be the reason for the rather weak effects of mutations on TPenA binding, we wanted to rule out the possibility that the detected affinity shifts only reflect allosteric effects on TPenA binding.

5.3 A double mutant shows direct interactions

We hypothesized that five of the identified residues interact directly with the blocker molecule, namely T157C, I182C, L189C, T266C and L304C. Independent, direct interaction of single residues with a bound molecule is reflected in the respective binding energy of the amino acid with it. In a double mutant, the loss of two residues that directly interact with TPenA would therefore result in the additive loss of their binding energies (Ren et al. 2012). On the other hand, two residues that both influence the same interaction with the blocker might each disrupt this interaction fully, therefore the respective double mutant would show no further loss in binding energy, or further increase in IC_{50}. In order to test the hypothesis of independent blocker interactions, two double mutants were designed.

First, a combination of both identified pore loop threonines, TREK-1 T157C-T266C was tested. However, this protein did not produce any measurable current. T157 and T266 together might be quintessential for ion conduction due to their proximity to the selectivity filter region: Only two residues upstream the GFG motif, these four introduced cysteines in close proximity to the selectivity filter are unlikely to allow potassium passage. While the dual mutant T157C-T266C did not produce measurable current under standard conditions, the double mutant T157C-L189C was

functional and showed an approximately 300-fold decrease in affinity with a TPenA IC_{50} of 4.4 ± 1.4 mM, compared to 14 ± 1.3 μM in the wild-type channel (Table 3, Fig. 9 b-c). In addition, the IC_{50} for THexA in this double mutant was 155 ± 9 μM, compared to 1 ± 0.4 μM in the wild-type channel.

As a result, the double mutant displayed rough but not absolute additivity. This might be partly explicable as a result of weak coupling energies due to structural rearrangements and compensations after mutant introduction (Horovitz 1996). However, we have to note that a double mutant with cysteines instead of alanines does not provide excellent conditions for such an analysis. With cysteine, it is rather likely that not only the investigated interaction of the original residue is removed, but that new, maybe relevant interactions are introduced into the protein, and that K_M might be affected by these interactions as well. In addition, the five above-mentioned residues forming the TPenA binding site were also tested for their impact on Fluoxetine and Amlodipine block in TREK-1. However, none of them had any effect on Fluoxetine or Amlodipine affinity compared to the wild-type channel, arguing strongly for a different inhibition mechanism for both molecules.

A TnA binding site inside the channel pore has been established in other K^+ channels before (Armstrong 1971, Yellen et al. 1991). Most notably, a crystal structure of a *KcsA* channel with a bound TBA molecule was published in 2001 (Zhou et al. 2001). In that structure, TBA binds directly beneath the selectivity filter, also interacting with conserved threonine residues within the filter motif. Furthermore, TBA is depicted to bind in a planar fashion, that means that all alkylic side chains lie in one plane. This conformation of TBA is also referred to as D_{2D}. On the other hand, the „octopus structure" does describe a TnA molecule, whose alkylic side chains are bent over, and whose diameter is therefore diminished. The correct conformation of the TnA molecule in the channel is relevant, as it defines the blocker molecule's planar diameter. Therefore, the set of pore lining residues that can interact with the blocker also depends on blocker conformation. As a consequence, the different TPenA conformations affect the conclusions that can be derived from experimental results concerning the channel's cavity diameter and the diameter of a putative cytosolic gate.

5.3 TPenA binds to TREK-1 in open and the closed states with equal affinity

As the putative binding site suggests a blocking mechanism working from within the pore, we performed experiments to demonstrate that TnA derivatives work as pore blockers rather than allosteric inhibitors. The demonstration of so-called tail currents is often used to prove, that a molecule acts as an ion channel pore blocker. It is based on the idea that a pore blocker can only enter its binding site if the channel cavity is open at the intracellular side. A second precondition is an open time constant of blocker binding (τ_{on}) which is slower than the opening of the channel's gate. This is necessary, as the channel must be allowed to open before subsequently being inhibited by the washed up blocker. With a sufficiently small τ_{on} the binding process of the blocker can then be observed as an exponentially decreasing current, also known as „transient current". This phenomenon can be seen in *Shaker* channels upon TnA block. As the inhibitor's open time constant is a product of the on rate k_{on} and the blocker concentration,

$$\tau_{on} = k_{on} \cdot [blocker]$$

τ_{on} can be reduced by reducing blocker concentration and therefore widening the time window to observe a transient current. However, to exploit this mechanism a high affinity blocker is mandatory. In TREK-1, THexA with an IC_{50} of 1 ± 0.4 µM is a high-affinity blocker and was therefore chosen to investigate the TnA blocking mechanism at a concentration of 1 µM. At this concentration, the τ_{on} was demonstrated to equal about 200 ms in TREK-1 (Piechotta et al. 2011). I performed this experiment with fast mechanoactivation of the TREK-1 channel. Fast pressure pulses were achieved by a high-speed pressure clamp, which was controlled via the EPC 10 system. Pressure pulses were transmitted directly via a connection between pressure clamp headstage and patch pipette holder. The τ_{on} for pressure activation was 25.5 ± 2.5 ms and therefore about ten times faster than the τ_{on} of 1 µM THexA. Using this approach, no transient current could be detected in the presence of THexA
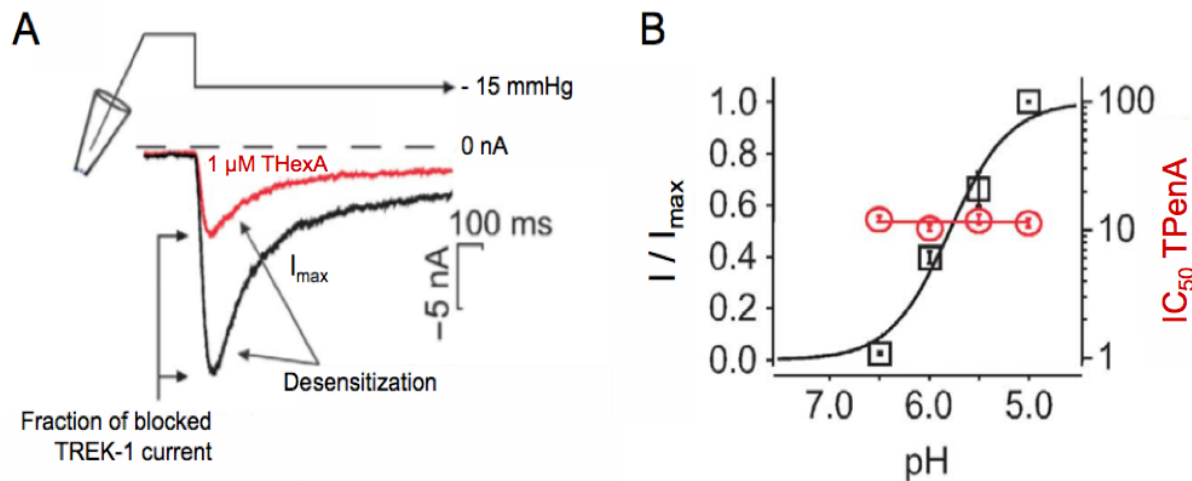
Figure 10. *TnA molecules can bind in open and closed TREK-1 channels with equal affinity*. (A) TREK-1 channels are mechanosensitive and can be activated by negative pressure. In this experiment, a continuous pulse of – 15 mmHg is applied to activate the channel in the absence (black) and presence of 1 µM THexA (red). A time-dependent desensitization is observed in both cases. (B) Changes in open probability of TREK-1 induced by cytosolic pH do not impact TPenA affinity.

(Fig. 10). Intriguingly, pressure activation of the TREK-1 current is followed by a slow desensitization of the channel with exponentially decreasing current. Therefore, this desensitization could be misinterpreted as tail current. However, this desensitization was present not only in the presence of THexA but also in blocker-free solution. Thus, it can be clearly distinguished from blocker-induced tail currents. Given the absence of tail currents, we rejected our first hypothesis of a cytosolic gate in TREK-1 and assumed, that TnA molecules bind to TREK-1 in both the open and the closed state of the channel with equal affinity. Consequentially, we hypothesized that changes in open probability would not affect blocker affinity expressed as IC_{50}.

In order to determine TPenA affinity's dependence on open probability, dose response curves were measured in different pH backgrounds. As a result, unlike voltage-gated potassium channels, open probability did not show any impact on blocker affinity (Fig. 10). This argues for a blocker that can enter its binding site without traversing any channel gate.

5.4 The pH-gate in TREK-1

Given the combined evidence of functional data and structural dockings, we posit that TnA derivatives act within the pore. The identified binding site shows that TnA act within the channel cavity as pore blockers. Therefore, the previous experiments show that the cytosolic BC gate, also referred to as „helix bundle crossing", is not functional in pH and pressure gating in TREK-1 channels.

With this cytosolic gate being constitutively open, the key conformational changes during gating must convene in another region of the protein, located „above" or rather on the extracellular side of the blocker binding site. With the selectivity filter already been proposed previously to be of importance for TREK-1 channel gating in response to extracellular pH (Cohen et al. 2008), an equally important function in intracellular pH and pressure gating seems to be likely.

Therefore we examined the impact of mutants in the selectivity filter region on pH gating. If pH gating was indeed enacted within the filter region, one would expect that mutagenetic perturbation of the channel filter, compromising its structural integrity, would shift the EC_{50} for pH gating. The filter region of TREK-1 is formed by ^{155}ITTIGFG^{161} in the first pore loop (P1) and ^{264}LTTIGFG^{270} in P2. Introducing mutants within the evolutionary conserved filter region does create a significant perturbation. We determined the EC_{50} values for activation by intracellular pH (pH_{ic}) in both filter regions, namely I155C to I158C and L264C to I267C. In TREK-1 wild-type channels, pH activation shows a biphasic behaviour. While the maximal activation requires an internal pH 5.0, a further increase in proton concentration leads to a partial inhibition of TREK-1 current, a so-called proton block (Fig. 11). Interestingly, all mutated residues showed significantly altered pH_{ic} EC_{50}. The most pronounced shifts were detected in the T157C mutant (Fig. 11).

Interestingly, in the double mutant T157C – L189C, pH sensitivity was abolished completely. However, it must be noted that beyond the filter regions, several scattered mutations also showed pronounced alterations regarding pH gating, notably A302C in the fourth transmembrane helix.
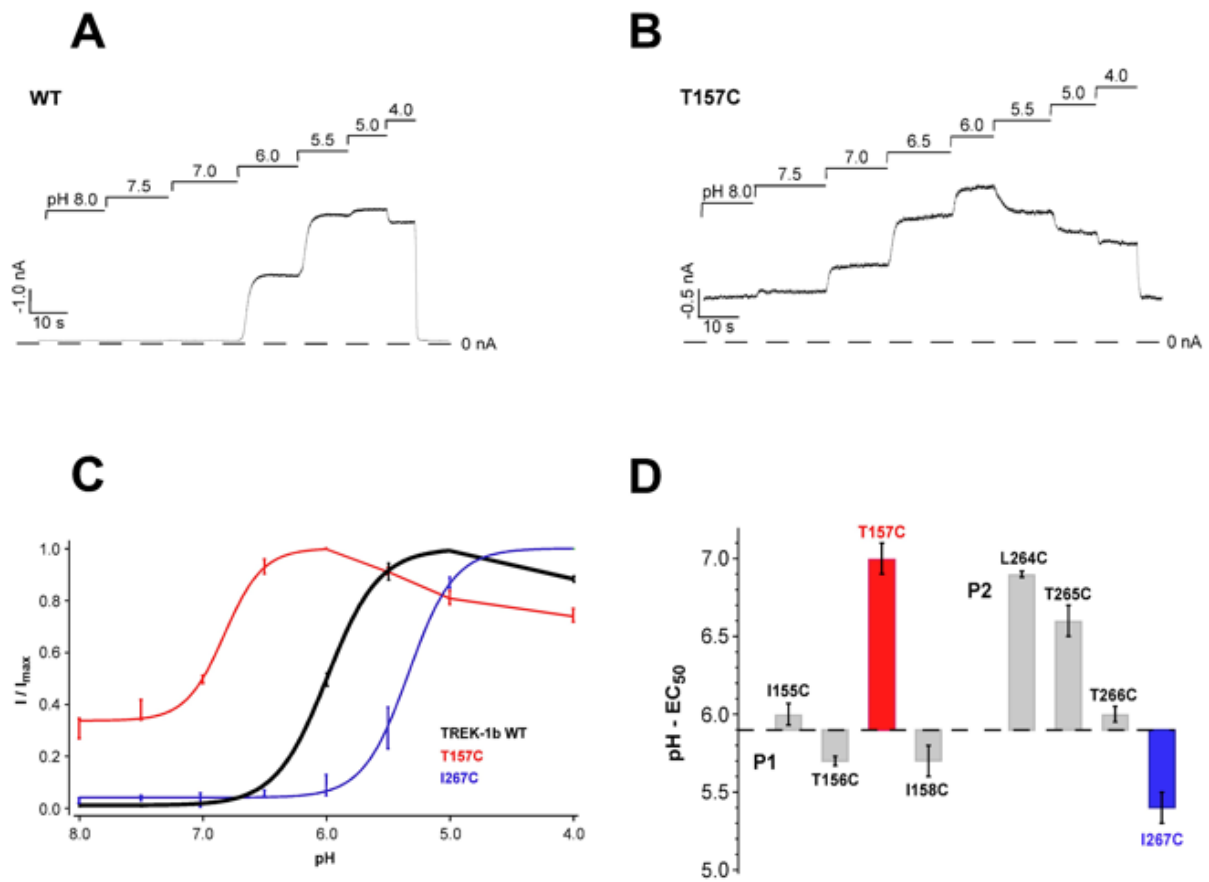
Figure 11. *pH-sensitive residues in the selectivity filter region.* (A) pH_{ic} activation in TREK-1 WT. (B) pH_{ic} activation in T157C. (C) Activation by intracellular pH fitted with a standard Hill equation for TREK-1 WT and the mutants T157C and I267C. (D) EC_{50} values for pH_{ic} activation in selectivity filter mutants of TREK-1.

Given these results, we can conclude that an important involvement of the filter region is present in pH gating, adding further evidence to the hypothesis of the selectivity filter acting as the channel gate in pH gating in TREK-1. Although we cannot rule out that the pH gate is located even above the selectivity filter in the pore loop region, we propose a gating model that is based on a collapsed, non-conductive selectivity filter as the closed state of the channel to be the most likely gating mechanism in TREK-1. This assumption is supported by this study as well as previous studies on extracellular pH gating in TREK-1 (Cohen et al. 2008).

6 Discussion

In this study, the pore and gating mechanisms in K2P channels were investigated. Employing a cysteine scan of the inner pore helices in the K2P member channel TREK-1, I characterized TnA derivatives as pore blockers in this potassium channel family. Subsequently, the binding of TnA derivatives was demonstrated to be independent of channel gating. This led to the conclusion that K2P channels, in contrast to other Potassium channel families like K_{ir} and K_v, do not employ a cytosolic helix bundle gate. Instead, their gating seems to rely solely on the selectivity filter region. Therefore, their gating mechanism differs markedly from other classical potassium channel families which employ at least two different gating mechanisms.

6.1 TnA block as a common feature in all K^+ channels

When K2P channels were described first, their insensitivity to classical potassium channel blockers was described as a major difference from K_v and K_{ir} channels. Molecules like 4-AP and Cs^+ did not block K2P channels (Fink et al. 1996, Fink et al. 1998). Extracellular TEA as a potent pore blocker in K_v and K_{ir} channels also failed to block K2P at micromolar concentrations (Fink et al. 1996). The effect of intracellular TEA and its derivatives on K2P had not been studied in detail.

In this study it is demonstrated that cytosolic TnA derivatives can block different K2P channel members at micromolar concentrations and voltage-independently (Fig. 6). Increasing side chain lengths of the symmetrical TnA blocker molecule resulted in blockers of higher affinity. In the studied K2P member channel TREK-1, this effect saturated for symmetrical TnA with a side chain length of six. Intriguingly, the same optimal side chain length was described for internal TnA block in hERG channels (Choi et al. 2011).

The TREK-1 binding site of TPenA as a TEA derivative was characterised utilising a cysteine scan that covers the inner helices of TREK-1 (Fig. 9). Five residues, namely T157, I182, L189, T266 and L304, were found to form the TPenA binding pocket in the upper channel cavity. It is located directly beneath the selectivity filter and

resembles the previously described TBA binding site in the *KcsA* channel (Zhou et al. 2001). Whereas both polar threonines, T157 and T266, are located centrally within the pore loop, the more lipophilic, nonpolar residues within this binding site are found peripherally in the transmembrane helices TM2 and TM2. Thus, the binding site echoes the structure of the blocker molecule with its central nitrogen and peripheral alkylic chains.

T157 and T266 are located only two residues upstream their respective selectivity filter motif glycine-phenylalanine-glycine (GFG). Therefore, their functional similarity in binding the symmetrical blocker TPenA indicates a possible structural symmetry between P1 and P2. Such a symmetry is known in classical potassium channels, but uncertain in K2P channels. In contrast to that, no hints of symmetry can be found between the two inner helices, neither in number nor in position of the identified residues. In the second transmembrane helix, only three mutants were demonstrated to shift TPenA affinity markedly, namely I182, P183 and L189. As TM2 spans from Q168 to G201, these three residues are located in the centre of the helix. Contrarily, twice as many mutants were singled out along the TM4 helix, with the majority of them in the distal half of it.

These differences in position and number of critical residues might be partly explicable by TM2 and TM4 serving different purposes: Unlike TM2, TM4 most likely translates C-terminal activation into conformational changes within the channel pore and the selectivity filter region. Mutants in TM4 might therefore be more likely to affect the channel's cavity and filter conformation. Interestingly, a small stretch of residues screened in the proximal C-terminus itself showed no effect on TPenA affinity.

Having identified the blocker binding site and the biophysical properties of TnA block it is possible to compare TnA block characteristics in TREK-1 and other K2P channels with those in K_{ir} and K_v channels. K_{ir} channels, upon intracellular TnA application, display remarkable voltage dependence, whereas TnA block is voltage-independent in K2P channels (Fig. 7). On the other hand, the properties of K_v channels are comparable to those in TREK-1: Voltage as well as extracellular K^+ concentrations hardly affect blocker potency. Based on that, one could hypothesize
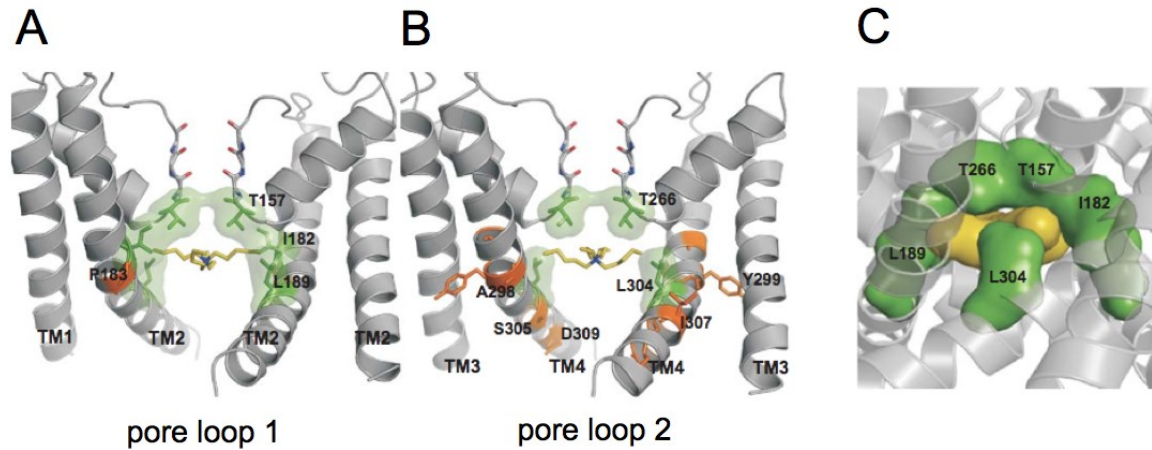
that K_v and K2P channels might share more pore and cavity properties than K2P and K_{ir} channels.

6.2 Pharmacological Implications

The described differences in blocker voltage dependency between K2P and K_{ir} channels could be exploited to elucidate K2P's role in different native cell types: The relative contributions of K_{ir} and K2P currents to the resting membrane potential are still unknown in the majority of native cell types. TnA molecules could serve as a molecular discriminator between both channel families. At hyperpolarized voltages and in the presence of TnA, only K2P channels would be blocked. K_{ir} channels, on the other hand, would still be conducting. Therefore, the contribution of the different channel classes to the resting membrane potential could be determined. As TnA molecules like TPenA and THexA have been shown to traverse the membrane (Choi et al. 2011), they could be applied extracellularly and still reach their binding site. Therefore, this approach might be feasible in whole-cell measurements.

6.3 Validating homology models with functional data

At the time of this study, no crystallized structure of any K2P channel had been published. Addressing this lack of information on K2P structure, molecular simulations based on the crystal structures of other K^+ channels tried to model K2P dimers in order to predict structural and functional characteristics of the protein (Maksaev et al. 2011, Kollewe et al. 2009, Streit et al. 2011). As further understanding of K2P architecture would greatly improve understanding of their structure-function relationship, one of the aims of this study was to test existing homology models for consistency with our functional data.

Figure 12. *The TPenA binding site is employed to evaluate homology models of the TREK-1 channel.* A TPenA molecule (yellow) is docked into the channel cavity with directly (green) and indirectly (orange) interacting residues. (A) Side-view highlighting relevant residues in P1 and TM2. (B) Side-view depicting relevant amino acids in P2 and TM4. (C) Surface model of the TPenA binding site. (D) Identification of the best-fit homology model for TREK-1. 18 homology models are tested for consistency with the functional data of this study regarding TPenA-interacting residues. Correct predictions of TPenA interactions are indicated in green, false-positives are symbolized by red signs. Residues with a presumed indirect interaction with TPenA are highlighted in yellow. MD simulations and model evaluation were performed by Dr. Phillip Stansfeld and Prof. Dr. Mark Sansom.

		in vitro	KvAP 1ORQ Open	MthK 3LDC Open	Kv1 2R9R Open	NaK 3E86 Open	KcsA 3FB6 Open 16	KcsA 3F7Y Open 17	KcsA 3FB8 Open 20	KcsA 3F5W Open 32	KcsA 3F7V Open 23	Model1 a Open	KcsA 3FB5 Open 14	KcsA 1K4C Closed	NaK 2AHY Closed	MlotiK 3BEH Closed	Model-2 b Closed	Model-3 b Closed	Model-4 b Closed	Model-5 a Closed
P1	T156																	✗	✗	
	T157	●	✓	✓	✓	✓	✓			✓	✓	✓		✓	✓	✓	✓	✓	✓	✓
	I158																			
TM2	I182	●	✓	✓	✓	✓	✓	✓	✓	✓		✓	✓	✓			✓	✓		
	P183	◌																		
	L184																		✗	✗
	F185			✗	✗			✗	✗	✗		✗		✗	✗	✗	✗	✗	✗	✗
	G186																	✗		
	F187																			
	L188																			
	L189	●		✓												✓		✓	✓	✓
	A190																			✗
P2	T265																	✗	✗	✗
	T266	●	✓	✓	✓	✓	✓	✓	✓	✓	✓	✓	✓			✓				✓
	I267																			
TM4	I293																✗	✗	✗	✗
	L294																		✗	
	V295																			
	G296	◌																		
	L297			✗	✗	✗	✗	✗	✗	✗	✗	✗	✗	✗		✗		✗	✗	✗
	A298	◌																		
	Y299	◌																		
	F300			✗	✗	✗	✗	✗	✗	✗	✗	✗	✗	✗	✗	✗				✗
	A301			✗	✗								✗	✗						
	A302																			
	V303																			
	L304	●	✓	✓				✓							✓					
	S305	●																		
	M306																			
	I307	◌																		
	G308																			
	D309	●																		
	W310																			

49

Having identified the TPenA binding site in TREK-1, this study's functional data regarding TPenA-interacting residues was employed by Phillip Stansfeld and Mark Sansom to evaluate the accuracy of 18 different homology models which had previously been derived (Fig. 12). Both closed and open state homology models were included: Closed state templates ranged from models based on the closed state crystal structures of *MlotiK*, *NaK* and *KcsA*, open state models included several *KcsA* structures as well as *KvAP*, *MthK*, Kv1.2. and *NaK*. Furthermore, two recently published TREK-1 models were included (Treptow und Klein 2010, Milac et al. 2011).

Consistency of the several tested models was evaluated by determining the number of correctly predicted amino acids interacting with a TPenA molecule, which was docked into the pore by aligning it with the coordinates of a TBA molecule in the *KcsA* crystal structure (Zhou et al. 2001). The respectable cut-off distance between blocker and amino acid side chain was set at four Ångström, any greater distance between amino acid and TPenA molecule was considered to disqualify as a possible interaction. In accordance with these conditions, the best fitting model was found to be the one based on a *KvAP* open channel structure. It correctly identified T157, I182, L189, T266 and L304 as interacting residues, without showing false-positives, that is, further interactions without functional correlate in our cysteine scan study (Fig. 11). Interestingly, this model represents an open state structure featuring four-fold symmetry. What is more, it revealed that the majority of residues identified in the fourth transmembrane helix do not affect TnA binding directly, but rather indirectly. This would be in conformity with the putative role of the TM4 segment, which is hypothesized to translate pressure and pH activation sensed or rather triggered at C-terminal domains into conformational changes within the gating structures of the channel filter.

6.4 Classical K$^+$ channel gating concepts and their role in TREK-1 channels

Over the past decades, three distinct gating concepts have been described for classical K$^+$ channels: „N-type" gating, „C-type" gating and so-called „bundle crossing" or BC gating as discussed above (Choi et al. 1991, Hoshi et al. 1991). It is

obvious that no N-type inhibition is present in K2P channels as they lack the N-terminal ball peptide structure. The roles of C- and BC-type gating are less clear. We argue, based on our functional data in TREK-1 channels and previous studies (Cohen et al. 2008), that a cytosolic bundle gate is not involved in K2P's pH gating and that pH gating in K2P channels relies on conformational changes within the selectivity filter.

TnA molecules played a pivotal role in determining the cytosolic BC gate in K_{ir} and K_v channels (Holmgren et al. 1997, Armstrong 1966, Armstrong 1971). Several observations employing TnA block in those channels led to the model of a gate that controls the intracellular entrance of the channel permeation pathway: Firstly, TEA block from the intracellular side requires an open channel: It was demonstrated that the blocker molecule can reach its binding site only in the open channel conformation (Armstrong 1971). Secondly, cytosolic TEA blockage was demonstrated to show higher efficacy at higher open probabilities (Choi et al. 1993). Thirdly, Armstrong could show that TEA derivatives like nonyltriethylammonium (TEA-C9) could be „trapped" within the channel cavity when applied from the intracellular side: The blocker would bind in the open state of the channel, was trapped during the closed state and would be released only after the channel had opened again. Based on these findings, it was assumed that cytosolic TEA must pass a cytosolic channel gate before it can reach its binding site. The blocker binding site was assumed to lie above this assumed gate, deeper within the channel cavity (Armstrong 1971). In sum, these experimental findings were seen as strong evidence for a cytosolic gate at the intracellular entrance into the channel cavity in K_{ir} and K_v channels.

As the TnA binding site in TREK-1 channels had been identified during this study and as TnA blockage in K2P resembles that in other potassium channel families, it was decided to employ TnA molecules to study the existence of an assumed cytosolic gate in K2P channels. In order to confirm a cytosolic gate, it was necessary to show first that TnA blockers can reach their binding site in K2P channels only when the channels are open.

In K_v channels without N-terminal ball peptides, a fast opening of the channel in the presence of THexA results in a so-called „transient current": Upon fast channel

opening e.g. by a voltage jump in the presence of THexA, the current is first fully activated and then inhibited exponentially by the blocker. This demonstrates that although the blocker is present before and after channel activation, it cannot bind until the channel switches to its open conformation. We performed similar experiments with TREK-1 channels. As TREK-1 is not voltage activated, fast channel activation was achieved by piezo-driven pressure clamp. THexA at 1 µM was used to ensure a small time constant τ_{on}. However, no tail currents could be observed (Fig. 10). Subsequent experiments by Dr. M. Bollepalli employing piezo-driven pH_{ic} activation could not yield any tail currents either. Consequently we assumed that pH gating and mechanogating do not involve a cytosolic gate in TREK-1.

The hypothesis of a cytosolic gate was therefore rejected. Consecutive experiments were designed to further prove the absence of a functional cytosolic gate in TREK-1 pH gating and mechanogating. For example, TnA affinity should not be affected by the channels's open probability if the blocker molecule does not need to traverse a gate before being able to enter its binding site. Contrarily, if a gate existed on the cytosolic side entrance of the channel, it would hinder blocker binding by prohibiting blocker binding during switches to at least one of the two closed states of the channel. In that case, a lower open probability would result in lower blocker affinity. Therefore, the affinity of the TPenA blocker at different open probabilities was measured (Fig. 10). Changes in open probability were induced by pH_{ic} changes. However, no changes in TPenA IC_{50} could be detected when measured separately in pH 5.0, 5.5, 6.0 or 6.5. Additionally, TnA molecules could not be trapped in the channel cavity, adding further evidence for the absence of a functional cytosolic channel gate. In summary, it can be stated that several experimental approaches, that led to the model of a cytosolic gate in K_v and K_{ir} channels, could not be reproduced in TREK-1 channels. Therefore we conclude that a cytosolic gate is not present in TREK-1 channels during pH gating and mechanogating.

If a cytosolic bundle gate does not exist in TREK-1 channels, other forms of gating must regulate these channels. As N-type gating is ruled out due to the above-mentioned reasons, only C-type gating provides a likely explanation for TREK-1 gating. Therefore, experiments were designed to positively confirm this hypothesis of a selectivity filter gate in TREK-1. If C-type gating acted as the primary gating

mechanism in TREK-1 channels, perturbations within or adjacent to the selectivity filter region should directly affect TREK-1 gating. Therefore, the impact of mutagenetic alterations within the filter regions on pH gating was investigated in this study (Fig. 11). As a result, all tested cysteine mutations within [155]ITTIGFG[161] in the first pore loop (P1) and [264]LTTIGFG[270] in the second pore loop (P2) shifted the pH EC_{50} either to higher or lower pH levels, thus supporting the hypothesis of a gating mechanism enacted within the selectivity filter region of the channel.

Additionally, the significance of the permeant ion on pH gating was evaluated. Stabilization of a K^+ channel filter by Rb^+ had been shown previously (Demo und Yellen 1992, Cuello et al. 2010b). To test, if similar results could be elicited from TREK-1 channels, Dr. M. Rapedius conducted experiments, in which a change of the permeating ion from K^+ to Rb^+ resulted in altered EC_{50} values for pH activation (Piechotta et al. 2011): The EC_{50} for pH_{ic} in symmetrical K^+ solutions equalling pH_{ic} 5.8 changed to approximately 8.0 in Rb^+ solutions. Contrarily, Tl^+ caused a small decrease in pH_{ic} EC_{50}, being consonant with findings that Tl^+ destabilises filter regions (Lu et al. 2001). The impact of both filter mutations on one hand and the influence of the permeating ion on pH_{ic} gating on the other hand strongly suggest a selectivity filter gate in TREK-1 pH_{ic} gating.

Intriguingly, two pore loop threonines T157 and T266 are part of the TPenA binding site in TREK-1. Thus, the binding site includes parts of the selectivity filter and putative gate, only one residue apart from the GFG filter motif. At first sight this might seem contradictory, because a channel gate must move and would therefore disrupt the optimal conformation of the binding site resulting in a TPenA affinity decrease. Such a decrease is actually not observed. However, the author would argue that the conformational changes exist and might even affect TnA binding, but the differences in free energy are too small to be observed in our experimental approach of giant inside-out patches.

Aside from the experimental evidence, the structure of TREK-1's inner helices TM2 and TM4 also supports the hypothesis of a lacking helix bundle gate in two-pore domain potassium channels. In K_v and K_{ir} channels, „hinge" motifs within the inner helices have been demonstrated to facilitate helix bundle gating (del Camino et al.

2000, Labro und Snyders 2012). These hinge regions enable the channel to bring its inner helices together in the lower third of the channel cavity and constrict the channel entrance. Both prolines and glycines can interrupt alpha helical structures and are therefore able to serve as the molecular basis for hinge regions. Whereas channels like *KcsA* with only two transmembrane helices per subunit (2TM-1P) rely on one single conserved glycine residue, K_v channels like the *Shaker* channel with six transmembrane helices per subunit possess an additional PXP motif about halfway through the pore-lining helix S6. In both channel superfamilies, these hinge regions have been demonstrated to enable significant movements of the inner helices and therefore a flexible cytosolic gate at the channel entrance (Labro und Snyders 2012).

K2P's inner helices resemble neither the structure of the S6 helix in K_v channels, nor classical TM2 architecture in K_{ir} channels. The inner helices TM2 and TM4 in K2P lack a PXP motif in both helices. Intriguingly, TM2 in TREK-1 contains five glycines and is therefore reminiscent of the inner helices in 2Tm-1P channels like *Kcsa* and *MthK*. In those channels, one glycine in the middle of each inner helix is sufficient to enable helix bundle crossing. However, TM4 in TREK-1 contains only two glycines, one of them close to the filter region (G296) and the second one at the cytosolic end of the helix (G308). No glycine is present in a more central position within the helix. Thus, no hinge motif is present in TM4.

Given the deviating architecture of the inner helices in K2P and therefore asymmetry between TM2 and TM4 it seems unlikely that a concerted movement of the inner helices could form a bundle crossing gate. In conclusion the author would argue, that a cytosolic bundle gate is not involved in TREK-1 pH gating and mechanogating.

6.5 A gating concept for TREK-1 channels

In the present study, a selectivity filter gating mechanism is proposed for pH_{ic} regulation and mechanogating in TREK-1 channels. The combined evidence of fast activation experiments, the lacking impact of open probability on TnA affinity, the abundance of residues in the filter region affecting pH_{ic} gating, the dependence of pH_{ic} gating on the permeating ion and the structural lack of symmetrical hinge regions suggests that the TREK-1 channel as a K2P member is constitutively open at the intracellular entrance of its channel cavity. We therefore hypothesize that pH_{ic} gating and mechanogating in TREK-1 take place within the selectivity filter region.

Recently, two crystal structures of the K2P channels TWIK-1 and TRAAK were published, representing the first crystal structures within the K2P family (Miller und Long 2012, Brohawn et al. 2012). As expected, both structures show channels that recapitulate the basic principles of K^+ channel architecture. They do so despite enormous differences in amino acid sequence when compared to other Potassium channel superfamilies. Both published crystal structures are so-called „open channel structures", meaning that the cytosolic entrance of the channel cavity is open with a diameter as wide as about ten Ångström. Additionally, the filter region in both crystallized K2P members shows fourfold symmetry despite several sequence differences between P1 and P2. Contrarily, the channel cavity displays only two-fold symmetry. In fact, the above-mentioned differences between TM2 and TM4 in K2P are crystallographically reflected in substantial conformational differences between the two helices: In TM2, the combination of several glycines and an additional proline halfway through the membrane generate a bend within the helix (Miller und Long 2012). The fourth transmembrane helix TM4, on the other hand, lacks any possible hinge motifs as described above. Correspondingly, in both crystal structures no bend can be observed within TM4 helices. In summary, with only two out of four helices of the dimeric channel presenting the structural prerequisites for helix bundle gating, the crystal structures argue once again in favour of an absent cytosolic gate.

Nevertheless, A. Miller and S. Long have argued that the results of the present study do not necessarily imply that K2P pH_{ic} gating only relies on the selectivity filter gate

(Miller und Long 2012). Their reasoning is mainly based on a surprising observation in the K2P crystal structures: Both TRAAK and TWIK-1 structures revealed unexpected side fenestrations of the channel cavity at the membrane-channel interface (Miller und Long 2012, Brohawn et al. 2012). These side fenestrations are a consequence of the structural differences between TM2 and TM4: The bend in TM2 results in different angles at which TM2 and TM4 traverse the membrane. As a result, an interhelical gap exists between the helices, possibly creating a direct passage between the channel cavity and the lipid bilayer. A. Miller and S. Long argue that this gap would suffice to allow any lipophilic TnA molecule like tetrahexylammonium (THexA) to enter its binding site within the channel cavity by diffusion through the membrane, bypassing any existing bundle crossing gate. However, several experimental results argue against THexA entering its binding pocket via channel side fenestrations:

THexA has been shown to be unable to block TREK-1 when applied extracellularly at concentrations up to 50 µM (Rapedius et al. 2012), arguing against the hypothesis of the blocker reaching its binding site by diffusing through the membrane. Contradictorily, it has been stated that TEA derivatives like THexA traverse the membrane by diffusion, but the respective study did not mention the concentrations at which TnA derivatives were applied extracellularly (Choi et al. 2011). Therefore, these results are still in accordance with the lack of a functional BC gate in TREK-1 and most likely other K2P channels.

As for now, the hypothesis of a lacking BC gate in TREK-1 channels has only been proven for the case of pH_{ic} gating. In the present study, pressure gating has not been scrutinized as extensively, mostly due to a lack of patches tolerating pressure application over a long period of time and strong desensitization in pressure-activated patches. Regarding lipid regulation, the lack of a functional BC gate during phospholipid gating in K2P has been demonstrated in a follow-up study (Rapedius et al. 2012).

Additionally, several results from other studies support a filter-based gating concept for K2P channels, with all activating stimuli converging in one conformational change taking place at the channel's selectivity filter. Firstly, possible links between the

different pathways have already been suggested, e.g. links between pressure and lipid gating on one hand or pressure and pH gating on the other hand (Patel et al. 1998b, Maingret et al. 1999, Honore et al. 2002b, Chemin et al. 2005b). Secondly, a study in 2001 by Zilberberg et al. provided evidence that in KCNKØ (or ORK1), a K2P channel in *Drosophila melanogaster*, all different conformational states of the channel can be influenced by alterations at the selectivity filter region or the adjacent outer pore (Zilberberg et al. 2001). Finally, a similar concept for channels relying solely on a selectivity filter gate has already been accepted for CNG channels (Contreras et al. 2008).

7 Conclusions

In this study on the structure-function relationship in TREK-1 channels as members of the K2P channel family, new insights into the pore structure and gating principles of two-pore domain K^+ channels are provided.

Firstly, TEA-derivatives (TnA) are described and characterized as novel K2P pore blockers. Secondly, the exemplary binding site of the TnA molecule tetrapentyl-ammonium (TPenA) is identified as being located directly beneath the channel's selectivity filter region in the channel pore. Identification of binding residues is achieved by employing a cysteine scan including transmembrane helices TM2 and TM4 as well as both filter regions and five residues in the C-terminal domain of TREK-1. Thirdly, TnA block in TREK-1 channels is characterised. It is demonstrated that blocker affinity increases with longer alkylic side chains. This effect saturates at alkylic side chains with six carbon atoms. Furthermore, TnA block in TREK-1 is found to be voltage-independent. Comparing these latter features to other K^+ channel subfamilies, TREK-1 channels resemble the TnA block characteristics of K_v, but not K_{ir} channels. Fourthly, the absence of a functionally relevant helix bundle gate in pH_{ic} gating and mechanogating is demonstrated in several experiments. It is shown that the TnA blocker molecule does not need to traverse a functional gate before entering its binding site during pH_{ic} gating or mechanogating. Consequentially, it is postulated that pH_{ic} gating in TREK-1 and other K2P channels relies solely on a selectivity filter gate.

With TnA blocking characteristics and the respective binding site being identified, it becomes possible to exploit TnA derivatives for further studies of K2P gating, characterising gating mechanisms in pressure, pH and lipid gating. Furthermore, the detected differences in gating and pore structures compared to other Potassium channel classes enhance the chance of developing drugs that affect the different kinds of Potassium channels more specifically.

References

Alloui A, Zimmermann K, Mamet J, Duprat F, Noel J, Chemin J, Guy N, Blondeau N, Voilley N, Rubat-Coudert C, Borsotto M, Romey G, Heurteaux C, Reeh P, Eschalier A, Lazdunski M. 2006. TREK-1, a K+ channel involved in polymodal pain perception. EMBO J, 25 (11):2368-2376.

Armstrong CM. 1966. Time course of TEA(+)-induced anomalous rectification in squid giant axons. J Gen Physiol, 50 (2):491-503.

Armstrong CM. 1971. Interaction of tetraethylammonium ion derivatives with the potassium channels of giant axons. J Gen Physiol, 58 (4):413-437.

Ashmole I, Goodwin PA, Stanfield PR. 2001. TASK-5, a novel member of the tandem pore K+ channel family. Pflugers Arch, 442 (6):828-833.

Bai X, Bugg GJ, Greenwood SL, Glazier JD, Sibley CP, Baker PN, Taggart MJ, Fyfe GK. 2005. Expression of TASK and TREK, two-pore domain K+ channels, in human myometrium. Reproduction, 129 (4):525-530.

Baker SA, Hennig GW, Han J, Britton FC, Smith TK, Koh SD. 2008. Methionine and its derivatives increase bladder excitability by inhibiting stretch-dependent K(+) channels. Br J Pharmacol, 153 (6):1259-1271.

Bang H, Kim Y, Kim D. 2000. TREK-2, a new member of the mechanosensitive tandem-pore K+ channel family. J Biol Chem, 275 (23):17412-17419.

Beckstein O, Tai K, Sansom MS. 2004. Not ions alone: barriers to ion permeation in nanopores and channels. J Am Chem Soc, 126 (45):14694-14695.

Berneche S, Roux B. 2001. Energetics of ion conduction through the K+ channel. Nature, 414 (6859):73-77.

Bockenhauer D, Zilberberg N, Goldstein SA. 2001. KCNK2: reversible conversion of a hippocampal potassium leak into a voltage-dependent channel. Nat Neurosci, 4 (5):486-491.

Brohawn SG, del Marmol J, MacKinnon R. 2012. Crystal structure of the human K2P TRAAK, a lipid- and mechano-sensitive K+ ion channel. Science, 335 (6067):436-441.

Buxton IL, Singer CA, Tichenor JN. 2010. Expression of stretch-activated two-pore potassium channels in human myometrium in pregnancy and labor. PLoS One, 5 (8):e12372.

Chavez RA, Gray AT, Zhao BB, Kindler CH, Mazurek MJ, Mehta Y, Forsayeth JR, Yost CS. 1999. TWIK-2, a new weak inward rectifying member of the tandem pore domain potassium channel family. J Biol Chem, 274 (12):7887-7892.

Chemin J, Patel A, Duprat F, Zanzouri M, Lazdunski M, Honore E. 2005a. Lysophosphatidic acid-operated K+ channels. J Biol Chem, 280 (6):4415-4421.

Chemin J, Patel AJ, Duprat F, Lauritzen I, Lazdunski M, Honore E. 2005b. A phospholipid sensor controls mechanogating of the K+ channel TREK-1. EMBO J, 24 (1):44-53.

Chen X, Aldrich RW. 2011. Charge substitution for a deep-pore residue reveals structural dynamics during BK channel gating. J Gen Physiol, 138 (2):137-154.

Choi KH, Song C, Shin D, Park S. 2011. hERG channel blockade by externally applied quaternary ammonium derivatives. Biochim Biophys Acta, 1808 (6):1560-1566.

Choi KL, Aldrich RW, Yellen G. 1991. Tetraethylammonium blockade distinguishes two inactivation mechanisms in voltage-activated K+ channels. Proc Natl Acad Sci U S A, 88 (12):5092-5095.

Choi KL, Mossman C, Aube J, Yellen G. 1993. The internal quaternary ammonium receptor site of Shaker potassium channels. Neuron, 10 (3):533-541.

Cohen A, Ben-Abu Y, Hen S, Zilberberg N. 2008. A novel mechanism for human K2P2.1 channel gating. Facilitation of C-type gating by protonation of extracellular histidine residues. J Biol Chem, 283 (28):19448-19455.

Contreras JE, Holmgren M. 2006. Access of quaternary ammonium blockers to the internal pore of cyclic nucleotide-gated channels: implications for the location of the gate. J Gen Physiol, 127 (5):481-494.

Contreras JE, Srikumar D, Holmgren M. 2008. Gating at the selectivity filter in cyclic nucleotide-gated channels. Proc Natl Acad Sci U S A, 105 (9):3310-3314.

Cordero-Morales JF, Cuello LG, Zhao Y, Jogini V, Cortes DM, Roux B, Perozo E. 2006. Molecular determinants of gating at the potassium-channel selectivity filter. Nat Struct Mol Biol, 13 (4):311-318.

Cotten JF, Zou HL, Liu C, Au JD, Yost CS. 2004. Identification of native rat cerebellar granule cell currents due to background K channel KCNK5 (TASK-2). Brain Res Mol Brain Res, 128 (2):112-120.

Cuello LG, Jogini V, Cortes DM, Perozo E. 2010a. Structural mechanism of C-type inactivation in K(+) channels. Nature, 466 (7303):203-208.

Cuello LG, Jogini V, Cortes DM, Pan AC, Gagnon DG, Dalmas O, Cordero-Morales JF, Chakrapani S, Roux B, Perozo E. 2010b. Structural basis for the coupling between activation and inactivation gates in K(+) channels. Nature, 466 (7303):272-275.

Danthi S, Enyeart JA, Enyeart JJ. 2003. Modulation of native TREK-1 and Kv1.4 K+ channels by polyunsaturated fatty acids and lysophospholipids. J Membr Biol, 195 (3):147-164.

del Camino D, Holmgren M, Liu Y, Yellen G. 2000. Blocker protection in the pore of a voltage-gated K+ channel and its structural implications. Nature, 403 (6767):321-325.

Demo SD, Yellen G. 1992. Ion effects on gating of the Ca(2+)-activated K+ channel correlate with occupancy of the pore. Biophys J, 61 (3):639-648.

Dillon DG, Bogdan R, Fagerness J, Holmes AJ, Perlis RH, Pizzagalli DA. 2010. Variation in TREK1 gene linked to depression-resistant phenotype is associated with potentiated neural responses to rewards in humans. Hum Brain Mapp, 31 (2):210-221.

Doyle DA, Morais Cabral J, Pfuetzner RA, Kuo A, Gulbis JM, Cohen SL, Chait BT, MacKinnon R. 1998. The structure of the potassium channel: molecular basis of K+ conduction and selectivity. Science, 280 (5360):69-77.

Duprat F, Lesage F, Fink M, Reyes R, Heurteaux C, Lazdunski M. 1997. TASK, a human background K+ channel to sense external pH variations near physiological pH. EMBO J, 16 (17):5464-5471.

Duprat F, Lesage F, Patel AJ, Fink M, Romey G, Lazdunski M. 2000. The neuroprotective agent riluzole activates the two P domain K(+) channels TREK-1 and TRAAK. Mol Pharmacol, 57 (5):906-912.

Eckert M, Egenberger B, Doring F, Wischmeyer E. 2011. TREK-1 isoforms generated by alternative translation initiation display different susceptibility to the antidepressant fluoxetine. Neuropharmacology, 61 (5-6):918-923.

Enyeart JA, Liu H, Enyeart JJ. 2008. Curcumin inhibits bTREK-1 K+ channels and stimulates cortisol secretion from adrenocortical cells. Biochem Biophys Res Commun, 370 (4):623-628.

Enyedi P, Czirjak G. 2010. Molecular background of leak K+ currents: two-pore domain potassium channels. Physiol Rev, 90 (2):559-605.

Fava M, Davidson KG. 1996. Definition and epidemiology of treatment-resistant depression. Psychiatr Clin North Am, 19 (2):179-200.

Fink M, Duprat F, Lesage F, Reyes R, Romey G, Heurteaux C, Lazdunski M. 1996. Cloning, functional expression and brain localization of a novel unconventional outward rectifier K+ channel. Embo Journal, 15 (24):6854-6862.

Fink M, Lesage F, Duprat F, Heurteaux C, Reyes R, Fosset M, Lazdunski M. 1998. A neuronal two P domain K+ channel stimulated by arachidonic acid and polyunsaturated fatty acids. EMBO J, 17 (12):3297-3308.

Girard C, Duprat F, Terrenoire C, Tinel N, Fosset M, Romey G, Lazdunski M, Lesage F. 2001. Genomic and functional characteristics of novel human pancreatic 2P domain K(+) channels. Biochem Biophys Res Commun, 282 (1):249-256.

Goldman DE. 1943. Potential, Impedance, and Rectification in Membranes. J Gen Physiol, 27 (1):37-60.

Gruss M, Mathie A, Lieb WR, Franks NP. 2004. The two-pore-domain K(+) channels TREK-1 and TASK-3 are differentially modulated by copper and zinc. Mol Pharmacol, 66 (3):530-537.

Hansen SB, Tao X, MacKinnon R. 2011. Structural basis of PIP2 activation of the classical inward rectifier K+ channel Kir2.2. Nature, 477 (7365):495-498.

Harinath S, Sikdar SK. 2004. Trichloroethanol enhances the activity of recombinant human TREK-1 and TRAAK channels. Neuropharmacology, 46 (5):750-760.

Heurteaux C, Guy N, Laigle C, Blondeau N, Duprat F, Mazzuca M, Lang-Lazdunski L, Widmann C, Zanzouri M, Romey G, Lazdunski M. 2004. TREK-1, a K+ channel involved in neuroprotection and general anesthesia. EMBO J, 23 (13):2684-2695.

Heurteaux C, Lucas G, Guy N, El Yacoubi M, Thummler S, Peng XD, Noble F, Blondeau N, Widmann C, Borsotto M, Gobbi G, Vaugeois JM, Debonnel G, Lazdunski M. 2006. Deletion of the background potassium channel TREK-1 results in a depression-resistant phenotype. Nat Neurosci, 9 (9):1134-1141.

Hodgkin AL, Huxley AF. 1947. Potassium leakage from an active nerve fibre. J Physiol, 106 (3):341-367.

Holmgren M, Smith PL, Yellen G. 1997. Trapping of organic blockers by closing of voltage-dependent K+ channels: evidence for a trap door mechanism of activation gating. J Gen Physiol, 109 (5):527-535.

Honore E, Maingret F, Lazdunski M, Patel AJ. 2002a. An intracellular proton sensor commands lipid- and mechano-gating of the K(+) channel TREK-1. EMBO J, 21 (12):2968-2976.

Honore E, Maingret F, Lazdunski M, Patel AJ. 2002b. An intracellular proton sensor commands lipid- and mechano-gating of the K+ channel TREK-1. Embo Journal, 21 (12):2968-2976.

Horovitz A. 1996. Double-mutant cycles: a powerful tool for analyzing protein structure and function. Fold Des, 1 (6):R121-126.

Hoshi T, Zagotta WN, Aldrich RW. 1991. Two types of inactivation in Shaker K+ channels: effects of alterations in the carboxy-terminal region. Neuron, 7 (4):547-556.

Humphrey W, Dalke A, Schulten K. 1996. VMD: visual molecular dynamics. Journal of molecular graphics, 14 (1):33-38, 27-38.

Ji XC, Zhao WH, Cao DX, Shi QQ, Wang XL. 2011. Novel neuroprotectant chiral 3-n-butylphthalide inhibits tandem-pore-domain potassium channel TREK-1. Acta Pharmacol Sin, 32 (2):182-187.

Kennard LE, Chumbley JR, Ranatunga KM, Armstrong SJ, Veale EL, Mathie A. 2005. Inhibition of the human two-pore domain potassium channel, TREK-1, by fluoxetine and its metabolite norfluoxetine. British Journal of Pharmacology, 144 (6):821-829.

Kim D, Gnatenco C. 2001. TASK-5, a new member of the tandem-pore K(+) channel family. Biochem Biophys Res Commun, 284 (4):923-930.

Kim Y, Bang H, Kim D. 2000. TASK-3, a new member of the tandem pore K(+) channel family. J Biol Chem, 275 (13):9340-9347.

Koh SD, Monaghan K, Sergeant GP, Ro S, Walker RL, Sanders KM, Horowitz B. 2001. TREK-1 regulation by nitric oxide and cGMP-dependent protein kinase. An essential role in smooth muscle inhibitory neurotransmission. J Biol Chem, 276 (47):44338-44346.

Kollewe A, Lau AY, Sullivan A, Roux B, Goldstein SA. 2009. A structural model for K2P potassium channels based on 23 pairs of interacting sites and continuum electrostatics. J Gen Physiol, 134 (1):53-68.

Labro AJ, Snyders DJ. 2012. Being flexible: the voltage-controllable activation gate of kv channels. Front Pharmacol, 3:168.

Lauritzen I, Chemin J, Honore E, Jodar M, Guy N, Lazdunski M, Jane Patel A. 2005. Cross-talk between the mechano-gated K2P channel TREK-1 and the actin cytoskeleton. EMBO Rep, 6 (7):642-648.

Lesage F, Terrenoire C, Romey G, Lazdunski M. 2000. Human TREK2, a 2P domain mechano-sensitive K+ channel with multiple regulations by polyunsaturated fatty acids, lysophospholipids, and Gs, Gi, and Gq protein-coupled receptors. J Biol Chem, 275 (37):28398-28405.

Lesage F, Guillemare E, Fink M, Duprat F, Lazdunski M, Romey G, Barhanin J. 1996. TWIK-1, a ubiquitous human weakly inward rectifying K+ channel with a novel structure. EMBO J, 15 (5):1004-1011.

Liu H, Enyeart JA, Enyeart JJ. 2007. Potent inhibition of native TREK-1 K+ channels by selected dihydropyridine Ca2+ channel antagonists. J Pharmacol Exp Ther, 323 (1):39-48.

Liu H, Enyeart JA, Enyeart JJ. 2009. N6-substituted cAMP analogs inhibit bTREK-1 K+ channels and stimulate cortisol secretion by a protein kinase A-independent mechanism. Mol Pharmacol, 76 (6):1290-1301.

Lu T, Wu L, Xiao J, Yang J. 2001. Permeant ion-dependent changes in gating of Kir2.1 inward rectifier potassium channels. J Gen Physiol, 118 (5):509-522.

MacKinnon R. 2004. Potassium channels and the atomic basis of selective ion conduction (Nobel Lecture). Angew Chem Int Ed Engl, 43 (33):4265-4277.

Maingret F, Honore E, Lazdunski M, Patel AJ. 2002. Molecular basis of the voltage-dependent gating of TREK-1, a mechano-sensitive K+ channel. Biochemical and Biophysical Research Communications, 292 (2):339-346.

Maingret F, Patel AJ, Lesage F, Lazdunski M, Honore E. 1999. Mechano- or acid stimulation, two interactive modes of activation of the TREK-1 potassium channel. J Biol Chem, 274 (38):26691-26696.

Maingret F, Patel AJ, Lesage F, Lazdunski M, Honore E. 2000a. Lysophospholipids open the two-pore domain mechano-gated K(+) channels TREK-1 and TRAAK. J Biol Chem, 275 (14):10128-10133.

Maingret F, Lauritzen I, Patel AJ, Heurteaux C, Reyes R, Lesage F, Lazdunski M, Honore E. 2000b. TREK-1 is a heat-activated background K(+) channel. EMBO J, 19 (11):2483-2491.

Maksaev G, Milac A, Anishkin A, Guy HR, Sukharev S. 2011. Analyses of gating thermodynamics and effects of deletions in the mechanosensitive channel TREK-1: comparisons with structural models. Channels (Austin), 5 (1):34-42.

Mazella J, Petrault O, Lucas G, Deval E, Beraud-Dufour S, Gandin C, El-Yacoubi M, Widmann C, Guyon A, Chevet E, Taouji S, Conductier G, Corinus A, Coppola T, Gobbi G, Nahon JL, Heurteaux C, Borsotto M. 2010. Spadin, a sortilin-derived peptide, targeting rodent TREK-1 channels: a new concept in the antidepressant drug design. PLoS Biol, 8 (4):e1000355.

Milac A, Anishkin A, Fatakia SN, Chow CC, Sukharev S, Guy HR. 2011. Structural models of TREK channels and their gating mechanism. Channels (Austin), 5 (1):23-33.

Miller AN, Long SB. 2012. Crystal structure of the human two-pore domain potassium channel K2P1. Science, 335 (6067):432-436.

Miller C. 1982. Bis-quaternary ammonium blockers as structural probes of the sarcoplasmic reticulum K+ channel. J Gen Physiol, 79 (5):869-891.

Milosavljevic N, Duranton C, Djerbi N, Puech PH, Gounon P, Lagadic-Gossmann D, Dimanche-Boitrel MT, Rauch C, Tauc M, Counillon L, Poet M. 2010. Nongenomic effects of cisplatin: acute inhibition of mechanosensitive transporters and channels without actin remodeling. Cancer Res, 70 (19):7514-7522.

Mongahan K, Baker SA, Dwyer L, Hatton WC, Park KS, Sanders KM, Koh SD. 2011. A Stretch-Dependent Potassium Conductance (TREK-1)and Its Function in Murine Myometrium. J Physiol.

Murbartian J, Lei Q, Sando JJ, Bayliss DA. 2005. Sequential phosphorylation mediates receptor- and kinase-induced inhibition of TREK-1 background potassium channels. J Biol Chem, 280 (34):30175-30184.

Namiranian K, Lloyd EE, Crossland RF, Marrelli SP, Taffet GE, Reddy AK, Hartley CJ, Bryan RM, Jr. 2010. Cerebrovascular responses in mice deficient in the potassium channel, TREK-1. Am J Physiol Regul Integr Comp Physiol, 299 (2):R461-469.

Nayak TK, Harinath S, Nama S, Somasundaram K, Sikdar SK. 2009. Inhibition of human two-pore domain K+ channel TREK1 by local anesthetic lidocaine: negative cooperativity and half-of-sites saturation kinetics. Mol Pharmacol, 76 (4):903-917.

Patel AJ, Honore E, Lesage F, Fink M, Romey G, Lazdunski M. 1999. Inhalational anesthetics activate two-pore-domain background K+ channels. Nat Neurosci, 2 (5):422-426.

Patel AJ, Honore E, Maingret F, Lesage F, Fink M, Duprat F, Lazdunski M. 1998a. A mammalian two pore domain mechano-gated S-like K+ channel. EMBO J, 17 (15):4283-4290.

Patel AJ, Honore E, Maingret F, Lesage F, Fink M, Duprat F, Lazdunski M. 1998b. A mammalian two pore domain mechano-gated S-like K+ channel. Embo Journal, 17 (15):4283-4290.

Perlis RH, Moorjani P, Fagerness J, Purcell S, Trivedi MH, Fava M, Rush AJ, Smoller JW. 2008. Pharmacogenetic analysis of genes implicated in rodent models of antidepressant response: association of TREK1 and treatment resistance in the STAR(*)D study. Neuropsychopharmacology, 33 (12):2810-2819.

Piechotta PL, Rapedius M, Stansfeld PJ, Bollepalli MK, Ehrlich G, Andres-Enguix I, Fritzenschaft H, Decher N, Sansom MS, Tucker SJ, Baukrowitz T. 2011. The pore structure and gating mechanism of K2P channels. EMBO J, 30 (17):3607-3619.

Rajan S, Wischmeyer E, Xin Liu G, Preisig-Muller R, Daut J, Karschin A, Derst C. 2000. TASK-3, a novel tandem pore domain acid-sensitive K+ channel. An extracellular histiding as pH sensor. J Biol Chem, 275 (22):16650-16657.

Rajan S, Wischmeyer E, Karschin C, Preisig-Muller R, Grzeschik KH, Daut J, Karschin A, Derst C. 2001. THIK-1 and THIK-2, a novel subfamily of tandem pore domain K+ channels. J Biol Chem, 276 (10):7302-7311.

Rapedius M, Schmidt MR, Sharma C, Stansfeld PJ, Sansom MS, Baukrowitz T, Tucker SJ. 2012. State-independent intracellular access of quaternary ammonium blockers to the pore of TREK-1. Channels (Austin), 6 (6):473-478.

Ren H, Zhao Y, Dwyer DS, Peoples RW. 2012. Interactions among positions in the third and fourth Membrane-associated domains at the intersubunit interface mf the N-Methyl-D-Aspartate Receptor Forming Sites of alcohol action. J Biol Chem.

Reyes R, Duprat F, Lesage F, Fink M, Salinas M, Farman N, Lazdunski M. 1998. Cloning and expression of a novel pH-sensitive two pore domain K+ channel from human kidney. J Biol Chem, 273 (47):30863-30869.

Sandoz G, Bell SC, Isacoff EY. 2011. Optical probing of a dynamic membrane interaction that regulates the TREK1 channel. Proc Natl Acad Sci U S A, 108 (6):2605-2610.

Sandoz G, Douguet D, Chatelain F, Lazdunski M, Lesage F. 2009. Extracellular acidification exerts opposite actions on TREK1 and TREK2 potassium channels via a single conserved histidine residue. Proc Natl Acad Sci U S A, 106 (34):14628-14633.

Sano Y, Inamura K, Miyake A, Mochizuki S, Kitada C, Yokoi H, Nozawa K, Okada H, Matsushime H, Furuichi K. 2003. A novel two-pore domain K+ channel, TRESK, is localized in the spinal cord. J Biol Chem, 278 (30):27406-27412.

Schmidt D, MacKinnon R. 2008. Voltage-dependent K+ channel gating and voltage sensor toxin sensitivity depend on the mechanical state of the lipid membrane. Proc Natl Acad Sci U S A, 105 (49):19276-19281.

Shin H-G, Xu Y, Lu Z. 2005. Evidence for sequential ion-binding loci along the inner pore of the IRK1 inward-rectifier K+ channel. The Journal of general physiology, 126 (2):123-135.

Streit AK, Netter MF, Kempf F, Walecki M, Rinne S, Bollepalli MK, Preisig-Muller R, Renigunta V, Daut J, Baukrowitz T, Sansom MS, Stansfeld PJ, Decher N. 2011. A specific two-pore domain potassium channel blocker defines the structure of the TASK-1 open pore. J Biol Chem, 286 (16):13977-13984.

Thomas D, Plant LD, Wilkens CM, McCrossan ZA, Goldstein SA. 2008. Alternative translation initiation in rat brain yields K2P2.1 potassium channels permeable to sodium. Neuron, 58 (6):859-870.

Thümmler S, Duprat F, Lazdunski M. 2007. Antipsychotics inhibit TREK but not TRAAK channels. Biochem Biophys Res Commun, 354 (1):284-289.

Tominaga M, Tominaga T. 2005. Structure and function of TRPV1. Pflugers Arch, 451 (1):143-150.

Treptow W, Klein ML. 2010. The membrane-bound state of K2P potassium channels. J Am Chem Soc, 132 (23):8145-8151.

Xian Tao L, Dyachenko V, Zuzarte M, Putzke C, Preisig-Muller R, Isenberg G, Daut J. 2006. The stretch-activated potassium channel TREK-1 in rat cardiac ventricular muscle. Cardiovasc Res, 69 (1):86-97.

Yamamoto Y, Hatakeyama T, Taniguchi K. 2009. Immunohistochemical colocalization of TREK-1, TREK-2 and TRAAK with TRP channels in the trigeminal ganglion cells. Neurosci Lett, 454 (2):129-133.

Yellen G, Jurman ME, Abramson T, MacKinnon R. 1991. Mutations affecting internal TEA blockade identify the probable pore-forming region of a K+ channel. Science, 251 (4996):939-942.

Zhou M, Morais-Cabral JH, Mann S, MacKinnon R. 2001. Potassium channel receptor site for the inactivation gate and quaternary amine inhibitors. Nature, 411 (6838):657-661.

Zhou M, Xu G, Xie M, Zhang X, Schools GP, Ma L, Kimelberg HK, Chen H. 2009. TWIK-1 and TREK-1 are potassium channels contributing significantly to astrocyte passive conductance in rat hippocampal slices. J Neurosci, 29 (26):8551-8564.

Zilberberg N, Ilan N, Goldstein SA. 2001. KCNKO: opening and closing the 2-P-domain potassium leak channel entails "C-type" gating of the outer pore. Neuron, 32 (4):635-648.

Zilberberg N, Ilan N, Gonzalez-Colaso R, Goldstein SA. 2000. Opening and closing of KCNKO potassium leak channels is tightly regulated. J Gen Physiol, 116 (5):721-734.

Appendix

Acknowledgement

Curriculum Vitae

name: Paula Louise Piechotta

date of birth: 19 September 1986

place of birth: Gera

Education

1993 – 1997   State primary school, Schmölln, Germany

1997 – 1999   State grammar school „Roman Herzog", Schmölln, Germany

1999 – 2006   State boarding school „Musikgymnasium Schloss Belvedere",
                    Weimar, Germany

10/2006 – 05/2014   Medical School, Friedrich Schiller University Jena, Germany

since 10/2012   M.Sc. Molecular Medicine, Friedrich Schiller University Jena,
                    Germany

Ehrenwörtliche Erklärung

Hiermit erkläre ich, dass mir die Promotionsordnung der Medizinischen Fakultät der Friedrich-Schiller- Universität bekannt ist,

ich die Dissertation selbst angefertigt habe und alle von mir benutzten Hilfsmittel, persönlichen Mitteilungen und Quellen in meiner Arbeit angegeben sind,

mich folgende Personen bei der Auswahl und Auswertung des Materials sowie bei der Herstellung des Manuskripts unterstützt haben: Prof. Dr. Thomas Baukrowitz, Dr. Markus Rapedius, Prof. Dr. Thomas Zimmer,

die Hilfe eines Promotionsberaters oder einer Promotionsberaterin nicht in Anspruch genommen wurde und dass Dritte weder unmittelbar noch mittelbar geldwerte Leistungen von mir für Arbeiten erhalten haben, die im Zusammenhang mit dem Inhalt der vorgelegten Dissertation stehen,

dass ich die Dissertation noch nicht als Prüfungsarbeit für eine staatliche oder andere wissenschaftliche Prüfung eingereicht habe und

dass ich die gleiche, eine in wesentlichen Teilen ähnliche oder eine andere Abhandlung nicht bei einer anderen Hochschule als Dissertation eingereicht habe.

Jena, den 23. Juni 2014   Paula Louise Piechotta, Verfasserin